AD-A195 327 ESTIMATING DEPTH OF CUT FROM BLADE FORCES ON THE ARMY 1/1
COUNTER OBSTACLE VEHICLE(U) MASSACHUSETTS INST OF TECH
CAMBRIDGE G B BAECHER APR 88 CERL-TR-P-88/11

UNCLASSIFIED F/G 8/10 NL

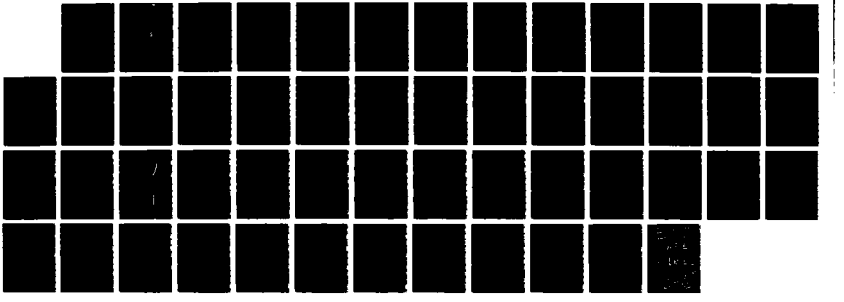

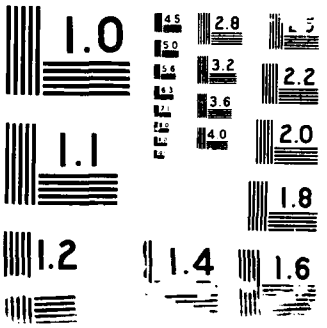
1.0
1.1
1.2
1.4
1.6
2.0
2.2
2.8
3.2
3.6
4.0
4.5
5.0

USA-CERL TECHNICAL REPORT P-88/11
April 1988

US Army Corps
of Engineers
Construction Engineering
Research Laboratory

Estimating Depth of Cut From Blade Forces on the Army Counter Obstacle Vehicle

The Counter Obstacle Vehicle (COV) is a heavyweight bulldozer-type vehicle used for earthwork and general obstacle removal in military operations. Microprocessor-based controls have been considered for use on the vehicle to automate blade control and thus enhance operator performance. This study evaluates the feasibility of using blade force measurements for controlling the depth of cut in real-time operation of the COV. This method of depth control is significantly limited because the variability of natural soil deposits causes the blade force to vary over time. To account for this, the study used random process (i.e., stochastic) models of soil variation based on empirical data to simulate natural deposits. Blade forces as the COV plowed through the simulated soils were calculated using soil mechanics models. Kalman filtering and optimal control techniques were used to adjust depth of cut based on measured blade force. Study results suggest the blade force variability may not be as great an obstacle to the use of force feedback for blade control as previously thought.

Unclassified
SECURITY CLASSIFICATION OF THIS PAGE

REPORT DOCUMENTATION PAGE

Form Approved
OMB No 0704 0188
Exp Date Jun 30 1986

1a REPORT SECURITY CLASSIFICATION
Unclassified

1b RESTRICTIVE MARKINGS

2a SECURITY CLASSIFICATION AUTHORITY

2b DECLASSIFICATION / DOWNGRADING SCHEDULE

3 DISTRIBUTION / AVAILABILITY OF REPORT
Approved for public release; distribution is unlimited.

4 PERFORMING ORGANIZATION REPORT NUMBER(S)
N/A

5 MONITORING ORGANIZATION REPORT NUMBER(S)
USA-CERL TR P-88/11

6a NAME OF PERFORMING ORGANIZATION
Massachusetts Institute of Technology

6b OFFICE SYMBOL (If applicable)

7a NAME OF MONITORING ORGANIZATION
U.S. Army Construction Engineering Research Laboratory

6c ADDRESS (City, State, and ZIP Code)
Cambridge, MA 02139

7b ADDRESS (City, State, and ZIP Code)
P.O. Box 4005
Champaign, IL 61820-1305

8a NAME OF FUNDING / SPONSORING ORGANIZATION
Belvoir Research (cont'd)

8b OFFICE SYMBOL (If applicable)
STRBE-JNC

9 PROCUREMENT INSTRUMENT IDENTIFICATION NUMBER
IAO DA 2544A6IL5, March 1986

8c ADDRESS (City, State, and ZIP Code)
Fort Belvoir, VA 22060

10 SOURCE OF FUNDING NUMBERS

PROGRAM ELEMENT NO	PROJECT NO	TASK NO	WORK UNIT ACCESSION NO

11 TITLE (Include Security Classification)
Estimating Depth of Cut From Blade Forces on the Army Counter Obstacle Vehicle (U)

12 PERSONAL AUTHOR(S)
Baecher, Dr. Gregory B., et al.

13a TYPE OF REPORT	13b TIME COVERED	14 DATE OF REPORT (Year, Month, Day)	15 PAGE COUNT
final	FROM _____ TO _____	1988, April	49

16 SUPPLEMENTARY NOTATION
Copies are available from the National Technical Information Service
Springfield VA 22161

17 COSATI CODES			18 SUBJECT TERMS (Continue on reverse if necessary and identify by block number)
FIELD	GROUP	SUB-GROUP	Counter Obstacle Vehicle, control systems, minesweepers, depth control, blades
19	03		
15	06	06	

19 ABSTRACT (Continue on reverse if necessary and identify by block number)

The Counter Obstacle Vehicle (COV) is a heavyweight bulldozer-type vehicle used for earthwork and general obstacle removal in military operations. Microprocessor-based controls have been considered for use on the vehicle to automate blade control and thus enhance operator performance. This study evaluates the feasibility of using blade force measurements for controlling the depth of cut in real-time operation of the COV. This method of depth control is significantly limited because the variability of natural soil deposits causes the blade force to vary over time. To account for this, the study used random process (i.e., stochastic) models of soil variation based on empirical data to simulate natural deposits. Blade forces as the COV plowed through the simulated soils were calculated using soil mechanics models. Kalman filtering and optimal control techniques were used to adjust depth of cut based on measured blade force. Study results suggest the blade force variability may not be as great an obstacle to the use of force feedback for blade control as previously thought.

20 DISTRIBUTION / AVAILABILITY OF ABSTRACT
☐ UNCLASSIFIED/UNLIMITED ☒ SAME AS RPT ☐ DTIC USERS

21 ABSTRACT SECURITY CLASSIFICATION
Unclassified

22a NAME OF RESPONSIBLE INDIVIDUAL	22b TELEPHONE (Include Area Code)	22c OFFICE SYMBOL
Jane Andrew	(217) 352-6511, x 388	CECER-IMT

DD FORM 1473, 84 MAR

83 APR edition may be used until exhausted
All other editions are obsolete

SECURITY CLASSIFICATION OF THIS PAGE
Unclassified

Block 8a. (Cont'd)

Development and Engineering Center (BRDEC)

FOREWORD

The work described in this report was performed for the Belvoir Research Development and Engineering Center (BRDEC) at Fort Belvoir under Intra-Army Order DA 2544A6IL5, dated March 1986. Under a contract administered by the U.S. Army Construction Engineering Research Laboratory, Facility Systems Division (USA-CERL-FS), the research was done by the Department of Civil Engineering at the Massachusetts Institute of Technology. The BRDEC Technical Monitor was Ms. Gloria Barrett (STRBE-JNC), and the USA-CERL point of contact was Mr. Robert Blackmon.

The authors would like to acknowledge the ideas and suggestions of Mr. Blackmon, which have improved this report and the direction of the project as a whole. The technical editor was Ms. Jane Andrew, USA-CERL Information Management Office.

COL Norman C. Hintz is Commander and Director of USA-CERL, and Dr. L. R. Shaffer is Technical Director. Dr. Michael J. O'Connor is Acting Chief, USA-CERL-FS.

CONTENTS

FIGURES

FIGURES (Cont'd)

TABLES

ESTIMATING DEPTH OF CUT FROM BLADE FORCES ON THE ARMY COUNTER OBSTACLE VEHICLE

1 INTRODUCTION

Background

Effective use of the Counter Obstacle Vehicle (COV) for minesweeping requires continuous plowing at a constant depth. However, because the COV encounters variations in ground topography as it moves along, the plow height must be continuously controlled to achieve a cut of constant depth. Since it is difficult for an operator to make such adjustments while closed inside the vehicle, automatic control is desirable.

The first requirement for such control is an accurate method for monitoring the position of the blade. For civilian vehicles, front mounted, exterior devices can be used to monitor blade position. As a combat vehicle, however, the COV operates in a hazardous environment where devices mounted on the exterior of the vehicle are vulnerable. The combat environment also precludes the use of visual inspections by the COV operators or other personnel.

An attractive alternative for blade control is real-time force feedback, by which the depth of cut is estimated from the force on the blade. However, the accuracy of blade control using force feedback depends on the accuracy with which plowing depth can be estimated from blade force. Such estimates are complicated by the dependence of blade force on (1) spatial variations of soil properties, (2) obstacles such as roots and boulders, and (3) dynamic effects of the blade passing through the soil.

Objective

The objective of this work was to assess the feasibility of using force feedback for controlling depth of cut of the COV blade. Controlling depth of cut depends primarily on the ability to accurately estimate depth at an arbitrary time from the time stream of blade forces measured up to and including that time. Thus, this work addressed the accuracy of depth of cut estimates made from blade forces.

Approach

To evaluate this method of estimation, a model was developed which is based on variations in the force on the blade which are caused by variations in the properties and topography of the soil. (The dynamic effects of the blade are not modeled.) To study the accuracy of the estimate produced using this model, several simulations were conducted.

The development of the overall model begins with a model of the forces on the blade (Chapter 2). These forces depend on the characteristics of the soil, and especially on the undrained shear strength, so that property is modeled using stochastic equations (Chapter 3). Since the ultimate goal is to use estimates of the force to control the position of the blade, a model of position and control is developed using stochastic control theory (Chapter 4). The final control function will require an estimate of the blade position, which can be obtained using the Kalman filter (Chapter 5). Finally all these elements, the force and soil models, the position equation from the control model (currently with zero external control), and the Kalman filter, are used to simulate the COV plowing operation.

2 BLADE LOAD MODEL

The principal plowing force on the COV blade results from shearing soil in front of the blade. The shearing strength of soil is usually modeled well by the Mohr-Coulomb failure criterion, expressed as[1]

$$\tau_f = c + \sigma_f \tan(\phi) \qquad \text{[Eq 1]}$$

where τ_f = shear stress on the failure surface
σ_f = normal stress on the failure surface
c = undrained soil strength (cohesion) and
ϕ = soil friction angle.

The soil parameters c and ϕ usually vary in space.

In pushing the blade into the soil, horizontal stresses in the soil mass increase until a failure surface develops. On this surface the stresses τ and σ satisfy the Mohr-Coulomb criterion (Figure 1).* The mechanics of blade action and soil failure in this pushing case are similar to passive failure of retaining structures. Considering two-dimensional equilibrium of the failed mass of soil, the force exerted on the blade can be expressed as[2]

$$F = 0.5\gamma d^2 N_\phi + 2cdN_c + qdN_q \qquad \text{[Eq 2]}$$

where F = force on the blade
γ = unit weight of soil
d = depth of cut
c = cohesion intercept
q = surcharge on the soil surface.

N_ϕ, N_c, and N_q are constants which depend on the soil friction angle and the blade's roughness. This force model is the sum of three terms. The first term is the contribution of lifting the failed mass up the failure surface, the second term is the undrained shearing of the soil, and the third term is the effect of surcharge.

Equation 2 is simple in form, but the variability of the soil parameters γ, c, N_ϕ, N_c, and N_q make the estimation of depth from force measurements impractical. Simplifications are necessary to apply this equation for the COV application.

Simplifying Assumptions

Smooth Blade

A smooth blade means that the soil exerts no lateral traction on the blade. Soil will not stick to the blade as it is plowed. Assuming low friction between the blade and soil, the parameters N_ϕ, N_c, and N_q simplify to functions of the soil friction angle.

---

[1]T. W. Lambe and V. R. Whitman, *Soil Mechanics* (John Wiley & Sons, New York, 1968).
*All tables and figures can be found at the end of this report (p 27).
[2]Lambe and Whitman.

$$N_\phi = \tan^2(45^\circ + \phi/2) \quad \text{[Eq 3]}$$

$$N_c = N_q = \tan(45^\circ + \phi/2) \quad \text{[Eq 4]}$$

and the failure surface is a plane inclined at $(45^\circ + \phi/2)$ from the vertical blade surface.

Undrained Condition

"Undrained condition" means that the soil is plowed quickly enough that water is not squeezed out of the soil during shearing. Thus, the water content of the soil is constant during plowing. If it is assumed that the soil is sheared at constant water content and that the blade is smooth, then Equation 1 reduces to $\tau = c$, and the blade load (Equation 2) becomes

$$F = 0.5\gamma d^2 + 2cd + qd \quad \text{[Eq 5]}$$

where the cohesion intercept, c, is the undrained shear strength. The assumption of undrained shearing of soil is reasonable for the COV operating at design plowing speeds or in low permeability soils such as silts and clays.

To examine the importance of each term in the force model expressed in Equation 2, a typical case was chosen with a blade depth of 2 ft* and loose soil in front of the blade. The geometry of this case is shown in Figure 2. Choosing typical c/γ ratios in the range 2 to 6, the contribution of each term as a percentage of total force is shown in Table 1.

At average strength values ($c/\gamma = 4$ to 5) the dominant term in the force function is the undrained shearing ($2cd$). As the depth increases, the contribution of the first term ($0.5\gamma d^2$) increases, but the limit on blade height places a physical limit on the magnitude of this term. For blade heights up to 4 ft, shearing is the dominant component of force. This observation can be interpreted to mean that for optimal control, variability in unit weight γ can be ignored compared to variability in shear strength: at typical operating depths (< 2 ft), random variations in unit weight result in insignificant changes of force. For example, at $c/\gamma = 4$, a 10 percent change in unit weight causes a 1 percent change in force.

Comparisons With Field Measurements

To confirm a force model similar to Equation 5 (with $q = 0$), O'Callaghan and McCullen performed full-scale bulldozer tests.[3] A dynamometer was mounted on the bulldozer blade and the force exerted on the blade was measured for various depths. Measured and calculated values of horizontal blade force are compared in Figure 3. The theoretical relationship is approximately linear, and thus satisfactory for present purposes, because of the insignificant contribution of the lift term ($0.5\gamma d^2$).

*A metric conversion table is provided at the end of this report (p 25).

[3]J. R. O'Callaghan and P. J. McCullen, "Soil Mechanics in Relation to Earth-Moving Machinery," *Institution of Mechanical Engineers—Proceedings* (Symposium on Earth-Moving Machinery), Vol 179, part 3F (1964-65), pp 23-29.

3 MODELING SOIL VARIABILITY

Covariance Function for Undrained Shear Strength

In the force model outlined in Chapter 2, the effects of soil are represented by γ, the unit weight and c, the undrained shear strength. The latter quantity, undrained shear strength of the soil, varies horizontally and vertically in any deposit, even those said to be homogeneous. This variability is usually modeled as a *second-order stochastic* field with statistical parameters estimated from field data.[4] A second-order stochastic field is similar to models used in other branches of science to represent fluctuating time-series of data (e.g., economics), only a stochastic field is defined in space rather than time and can be defined over multiple dimensions. Stochastic field models are used to characterize the spatial variability of soils because no amount of field testing can ever completely characterize the point-to-point variation of natural soils.

A second-order, stationary, random process is completely specified by a mean (or mean trend) and a covariance function. The function describes the degree of covariance between soil properties as a function of separation in space. For a stationary process, the covariance between any two points depends only on the (vector) separation between points and not on their location within the domain. Thus, the covariance function is the same everywhere. Experience with undrained shear properties of natural soils has demonstrated that the covariance function can be adequately modeled as an exponential function of the form

$$B(r) = \sigma^2 e^{-r/r_o} \qquad \text{[Eq 6]}$$

where $B(r)$ = covariance function evaluated at separation r
σ^2 = variance of the fluctuations around the mean
r_o = a scale parameter called the covariance distance
r = separation between any two points.

Empirically, the covariance distance r_o is usually anisotropic, shorter by a factor of about 10 in the vertical compared to horizontal direction.

De Groot used a maximum likelihood method to estimate the covariance parameters, σ^2 and r_o, for several natural soil deposits. His results suggest that horizontal covariance distances in different soil deposits can vary from 50 to 200 ft and that coefficients of variation (standard deviation divided by mean) range from 15 to 35 percent. These results are consistent with the findings of others.[5]

---

[4] D. J. DeGroot, "Maximum Likelihood Estimation of Spatially Correlated Soil Properties," M.S. Thesis, M.I.T., May 1985.

[5] G. B. Baecher, et al., "Geotechnical Reliability of Offshore Gravity Platforms," M.I.T. Sea Grant, Report MITSG 80-20, Cambridge, MA, 1980; Spikula, D., "Statistical Estimation of Soil Properties: An Application," M.S. Thesis, M.I.T., May 1983; W. Tang, "Probabilistic Evaluation of Penetration Resistance," *American Society of Civil Engineers Journal, Geotechnical Engineering Division*, Vol 105, GT10 (1979) pp 1173-1191.

Covariance functions and coefficients of variation reported in the literature usually refer to point properties measured in individual tests or at specific depths in a boring. As such, they summarize the stochastic variability among small elements of soil. A blade, on the other hand, moves soil within a much larger volume. Variations in blade load are related to variations among the average properties of such larger soil volumes. Since variations from point to point within these larger volumes are averaged, the coefficient of variation of volume-averaged properties is reduced compared to those of point properties. At the same time, the covariance function is spread out, giving larger covariance distances.

The reduction of variability with volume and the spreading of the covariance function is counteracted by discrete changes in soil type that may occur along the path of plowing. Soil properties across such discrete changes have little correlation with one another, and thus both increase the volume-averaged coefficient of variation and decrease the covariance distance.

In the simulation studies it was decided to strike a balance between these opposing trends by adopting a coefficient of variation of 10 percent and a covariance distance, r_o, of 50 ft. Choosing a typical average undrained shear strength of 400 psf, the stochastic behavior of the undrained shear strength can be completely specified by its first and second moments:

$$E[c] = 400 \text{ psf} \qquad \text{[Eq 7]}$$

$$B_{cc}(r) = 1600e^{-r/50} \qquad \text{[Eq 8]}$$

where E = the expectation (i.e., mean or arithmetical average)
r = the separation in feet.

Stochastic Differential and Difference Equations for Undrained Shear Strength

Optimal stochastic control (discussed in Chapter 4) requires that random processes must be specified in stochastic differential or difference form. One of the many stochastic processes of this form is the first-order Gauss-Markov process, which is a normal or Gaussian process with an exponential covariance function. The covariance function of the undrained shear strength of soil (Equation 6) is also exponential, so it is assumed that the undrained shear strength, like the Gauss-Markov, is a normal process. Therefore, its behavior can be described by a stochastic differential equation for a normal process:[6]

$$dc/dt = -(1/r_o)c + (1/r_o)E[c] + \epsilon \qquad \text{[Eq 9]}$$

where c = undrained shear strength of the soil
r_o = covariance distance of the undrained shear strength of the soil.

[6] A. Gelb, *Applied Optimal Estimation* (M.I.T. Press, Cambridge, MA, 1974).

In Equation 9, ϵ is Gaussian white noise with

$$E[\epsilon] = 0 \qquad \text{[Eq 10]}$$

$$E[\epsilon^2] = (2/r_o)\sigma^2_c \qquad \text{[Eq 11]}$$

where E = the expectation operator
r_o = the covariance distance of the undrained shear strength of the soil
σ^2_c = the variance.

In discrete time Equation 9 can be written as a stochastic difference equation,

$$c(t+1) = \Psi c(t) + v(t) \qquad \text{[Eq 12]}$$

where $v(t)$ is an independent Gaussian sequence, and from Gelb and Equations 7 and 8,

$$\Psi = e^{-1/r_o} = 0.98 \qquad \text{[Eq 13]}$$

$$E[v^2] = \sigma^2_c(1 - \Psi^2) = 62.7. \qquad \text{[Eq 14]}$$

4 BASICS OF STOCHASTIC CONTROL THEORY

Stochastic control theory deals with dynamic systems whose states are described by stochastic differential or difference equations. For example, simple stochastic control involves a linear system disturbed by Gaussian white noise. Linearity refers to measurements, $\underline{y}(t)$, of the system state, $\underline{x}(t)$, which depend linearly on the values of $\underline{x}(t)$. White noise refers to variations in the state variables, $\underline{x}(t)$, which are independent and identically distributed for different values of t. The objective of this theory below is to determine a function [$\underline{u}(t)$ below] that will "control" the state of the system [described by $\underline{x}(t)$] so as to minimize the deviations of that state from some ideal value or set of values. There are two cases to be considered: the ideal case, where measurements of the state of the system, $\underline{x}(t)$, are exact, thus the only noise is the Gaussian white noise, $\underline{w}(t)$; and the "noisy" case, where observations of the system, $\underline{y}(t)$, contain noise $\underline{v}(t)$, in addition to white noise. The derivations below address both cases.

System with White Noise Only

In the first case it is presumed that the initial conditions are random, but that the state of the system can be measured with complete certainty at any time. The system can be represented by the equation

$$\underline{x}(t+1) = \Psi\underline{x}(t) + \Gamma\underline{u}(t) + \underline{w}(t) \qquad \text{[Eq 15]}$$

where $\underline{x}$ = n-dimensional state vector
$\underline{u}$ = m-dimensional control vector
$\underline{w}$ = n-dimensional vector of random perturbations
Ψ = n*n one-step transition matrix from $\underline{x}(t)$ to $\underline{x}(t+1)$
Γ = n*m one-step transfer matrix from $\underline{u}(t)$ to $\underline{x}(t+1)$.

By the Gaussian white noise assumption, the random vectors $\underline{w}(0)$, $\underline{w}(1)$,...., $\underline{w}(t)$ are independent, with mean $E[\underline{w}(t)]$ and covariance $E[\underline{w}(t)\,\underline{w}^T(t)]$ having values,

$$E[\underline{w}(t)] = \underline{0}, \quad E[\underline{w}(t)\,\underline{w}^T(t)] = Q \qquad \text{[Eq 16]}$$

where T is the transpose. The initial condition $\underline{x}(0)$ is taken to be unknown, but with specified mean $E[\underline{x}(0)]$ and covariance matrix $E[\underline{x}(0)\underline{x}^T(0)]$ having the values,

$$E[\underline{x}(0)] = \underline{0}, \quad E[\underline{x}(0)\,\underline{x}^T(0)] = P_o \qquad \text{[Eq 17]}$$

The control procedure attempts to minimize deviations of the process $\underline{x}(t)$ from some ideal value or trajectory of values. Without loss of generality, these ideal values are set to zero. For practical reasons, squared deviations of $\underline{x}(t)$ from the ideal values $\underline{x}(t) = \underline{0}$ are frequently chosen to be minimized. This leads to a performance criterion, J, of the quadratic form,

$$J = E\{\Sigma[\underline{x}^T(t)A\underline{x}(t) + \underline{u}^T(t)B\underline{u}(t)]\} \qquad \text{[Eq 18]}$$

where A and B are positive definite matrices which express the cost of deviations of the components of $\underline{x}(t)$, and the cost of controls, respectively. Mathematically, the

matrices A and B are arbitrary. Quantitative values for A and B depend on the application in question.

Because this "ideal" situation is identical to a deterministic control problem, the controller $\underline{u}(t)$ which minimizes J (Equation 18) is[7]

$$\underline{u}(t) = -L\underline{x}(t) \qquad \text{[Eq 19]}$$

where L, the feedback matrix, depends on Ψ, Γ, A, and B.

System with Additive Noise

For most optimal control problems, including force feedback for the COV, the state variables, $\underline{x}(t)$, are observed indirectly and with measurement errors. Let $\underline{y}(t)$ be the vector of observations of the states $\underline{x}(t)$; then

$$\underline{y}(t) = \underline{g}(\underline{x}(t)) + \underline{v}(t) \qquad \text{[Eq 20]}$$

where $\underline{g}(.)$ = a deterministic function
$\underline{v}(t)$ = a vector of independent, identically distributed (iid) measurement errors.

In the blade control problem, the function $\underline{g}(\underline{x}(t))$ is the blade load model of Equation 5, or a linearized version of it. The state vector comprises blade depth and undrained shear strength. In most cases $\underline{g}(t)$ is a linear function (discussed in the next section) such that Equations 15 and 20 lead to the system of equations,

$$\begin{aligned} \underline{x}(t+1) &= \Psi\underline{x}(t) + \Gamma\underline{u}(t) + \underline{w}(t) \\ \underline{y}(t) &= H\underline{x}(t) + \underline{v}(t) \end{aligned} \qquad \text{[Eq 21]}$$

where H is the deterministic matrix of coefficient terms expressing the linear function $\underline{g}(.)$, and $\underline{w}(t)$ and $\underline{v}(t)$ are independent Gaussian white noise sequences with moments

$$\begin{aligned} E[\underline{w}(t)] &= 0, \quad & E[\underline{w}(t)\,\underline{w}^T(t)] &= Q \\ E[\underline{v}(t)] &= 0, \quad & E[\underline{v}(t)\,\underline{v}^T(t)] &= R \end{aligned} \qquad \text{[Eq 22]}$$

and $\underline{x}(0)$ is a Gaussian vector, independent of $\underline{v}(t)$ and $\underline{w}(t)$, with properties defined in Equation 17.

[7] A. E. Bryson and Y. C. Ho, *Applied Optimal Control* (Blaisdell Publishing Co., Waltham, MA, 1969).

The optimal controller for the system of Equation 21, given the performance criterion of Equation 18, is[8]

$$\underline{u}(t) = - L\underline{\hat{x}}(t) \qquad \text{[Eq 23]}$$

where L = the feedback matrix
$\underline{\hat{x}}(t)$ = the mean estimate of $\underline{x}(t)$ conditioned on the measurements $\underline{y}(0), \underline{y}(1), \ldots, \underline{y}(t)$.

The estimate $\underline{\hat{x}}(t)$ is used as if it were exact, similar to deterministic control.

The solution of Equation 23 results from the so-called "separation theorem."[9] This theorem holds that stochastic control problems with a quadratic performance criterion (e.g., Equation 18) can be separated into two independent parts: one is an optimal filter by which $\underline{\hat{x}}(t)$ is estimated from the observations $\underline{y}(t)$; the other is linear feedback from the estimated state, $\underline{\hat{x}}(t)$, obtained in the same way as in the case of no observation errors.

The process by which $\underline{\hat{x}}(t)$ is estimated is based on Kalman filtering. The filter is recursive and depends *only on the system dynamics and noise characterization.* The estimate $\underline{\hat{x}}(t)$ is independent of the quadratic performance criterion J. Thus, controlled behavior for a dynamic system depends to a large extent on the performance of the Kalman filter. As a result, a major portion of this feasibility analysis has concentrated on the adequacy of Kalman filter estimation of depth from the time stream of the blade load.

Nonlinear Observations

In many physical systems, including the blade load model of Equation 5, the observation vector $\underline{y}(t)$ is a nonlinear function of the state variables $\underline{x}(t)$. To obtain practical solutions, the nonlinear function $\underline{g}(.)$ can be made linear by expanding it in a Taylor series around a known vector, for example, the expected value of $x(t)$.[10] Filtering and control operations are performed on this linearized system. This approach is used in Chapter 6, where the blade load model is linearized around the desired depth of cut and the mean undrained shear strength.

---

[8]K. J. Astrom, *Introduction to Stochastic Control Theory* (Academic Press, New York, NY, 1970).
[9]K. J. Astrom.
[10]A. Gelb.

5 KALMAN FILTER - THEORY AND RESULTS

This section summarizes rudimentary Kalman filter theory as applied to the estimation of blade depth from force measurements. The Kalman filter is used to estimate the conditional mean of the state variables, $\hat{x}(t)$, from which the controller is calculated as in Equation 23. Clearly, the accuracy of the control signal $\underline{u}(t)$ and the behavior of the controlled system $\underline{x}(t)$ depend on the accuracy with which $\underline{\hat{x}}(t)$ is estimated.

Force on the blade is a function of two random variables, the undrained shear strength of the soil being plowed and the depth of cut. The greater the soil strength and the deeper the cut, the greater the force. The force feedback system simultaneously estimates two unknowns and makes adjustments to (i.e., controls) the blade accordingly. The extent to which the depth of cut at time t+1 can be precisely controlled depends on the capability of the filter to adequately estimate the existing depth of cut at time t. This estimate is hindered by random variations of the undrained shear strength and inaccuracies in the model $\underline{g}(.)$.

Kalman Filter

Kalman filtering arises in many engineering problems where an estimation algorithm is required to sequentially process observations of a dynamic system. Since their development in the early 1960s,[11] the properties of the Kalman filters have been well studied.

From Equation 15 the process equation for an uncontrolled system is

$$\underline{x}(t+1) = \Psi\underline{x}(t) + \underline{w}(t) \qquad \text{[Eq 24]}$$

where $\underline{x}(t)$ = the state vector at time t
Ψ = a transition matrix
$\underline{w}(t)$ = a vector of iid perturbations (i.e., white noise).

The state $\underline{x}(t)$ is observed by noisy measurements (the observation includes additive noise):

$$\underline{y}(t) = H\underline{x}(t) + \underline{v}(t) \qquad \text{[Eq 25]}$$

where $\underline{y}(t)$ = the observation vector
H = a deterministic matrix
$\underline{v}(t)$ = a vector of iid observation errors.

[11] R. E. Kalman, "A New Approach to Linear Filtering and Prediction Problems," *American Society of Mechanical Engineers (ASME) Journal of Basic Engineering*, Vol 82 (1960), pp 34-45; R. E. Kalman and R. S. Bucy, "New Results in Linear Filtering and Prediction Theory," *ASME Journal of Basic Engineering*, Vol 83 (1961), pp 95-107.

The initial state $\underline{x}(0)$, perturbations $\underline{w}(t)$, and measurement errors $v(t)$ are assumed to be uncorrelated, with moments

$$E[\underline{x}(0)] = 0, \qquad E[\underline{x}(0)\underline{x}(0)^T] = P_o$$

$$E[\underline{w}(t)] = \underline{0}, \qquad E[\underline{w}(t)\underline{w}(t)^T] = Q \qquad \text{[Eq 26]}$$

$$E[\underline{w}(t)] = \underline{0}, \qquad E[\underline{v}(t)\underline{v}(t)^T] = R$$

The Kalman filter can be obtained as the linear Bayes' least squares estimate of the state vector $\underline{x}(t)$, given the observations $\underline{y}(0)$, $\underline{y}(1)$,.....,$\underline{y}(t)$.[12] To indicate the time at which an estimate of $x(t)$ is made--because different amounts of information are available at different times--let the estimate conditional on observations up to time t be denoted $\hat{x}(t/t)$, rather than $\hat{\underline{x}}(t)$ as used in the previous section. In this manner, an estimate conditioned on observations up to time $(t-1)$ would be denoted $\hat{\underline{x}}(t/t-1)$. The equations of the Kalman filter can be written as

$$\hat{\underline{x}}(t/t) = \hat{\underline{x}}(t/t-1) + K(t)[\underline{y}(t) - H\hat{\underline{x}}(t/t-1)] \qquad \text{[Eq 27]}$$

where $\hat{\underline{x}}(t/t-1)$ = estimate of $\underline{x}(t)$, given $\underline{y}(t-1)$

$$= \Psi\hat{\underline{x}}(t-1/t-1) \qquad \text{[Eq 28]}$$

$K(t)$ = Kalman gain matrix

$$= P(t/t-1)H^T\{H[P(t/t-1)]H^T + R\}^{-1} \qquad \text{[Eq 29]}$$

where H = matrix relating the measurements $\underline{y}(t)$ to the measured state variables $\underline{x}(t)$,

$P(t/t-1)$ = covariance matrix of the estimate $\hat{\underline{x}}(t/t-1)$ in Equation 28

$$= [P(t-1/t-1)]\Psi^T + Q \qquad \text{[Eq 30]}$$

$P(t/t)$ = covariance matrix of the estimate $\underline{x}(t/t)$ in Equation 27

$$= (I - K(t)H)[P(t/t-1)] \qquad \text{[Eq 31]}$$

where I is the identity matrix.

The Kalman filter is recursive in that the estimate of the state variable at time t, $\hat{\underline{x}}(t/t)$, is completely defined from the observation vector $\underline{y}(t)$ and the previous step estimate $\hat{\underline{x}}(t-1/t-1)$. At time zero, the covariance matrix of $\underline{x}(0)$ is given by Equation 26. This is used to calculate the covariance matrix of the first time step estimate before a measurement is made, P(1/0), using Equation 30. The covariance matrix after the first measurement is made, P(1/1), is calculated using Equation 31. Subsequent covariance matrices up to P(t/t) are calculated by recursive application of Equations 30 and 31.

[12] A. Gelb.

This recursive property reduces computation and computer memory requirements. Also, the estimate variances and covariances of Equations 29 through 31 are independent of the estimates in Equations 27 and 28. This means that covariance matrices and filter gains can be calculated in advance and stored in the computer system. Thus, the recursive calculations do not have to be made while the system is in operation (i.e., while the COV is moving), thus real-time application of the Kalman filter is enhanced.

Kalman Filter Applied to a Linear, Scalar System

To illustrate the performance of Kalman filters for simple system dynamics, a series of simulations were performed. The system model was taken as linear and scalar:

$$\underline{x}(t+t) = \Psi\underline{x}(t) + \underline{w}(t)$$
$$\underline{y}(t) = \underline{x}(t) + \underline{v}(t) \qquad \text{[Eq 32]}$$

where the notation follows that of Equations 15 and 20.

Let the covariance function of x be

$$B_{xx}(r) = \sigma_x^2 \, e^{-r/r_o} \qquad \text{[Eq 33]}$$

where $B_{xx}(r)$ = the covariance of $x(i)$, $x(i+r)$
σ_x^2 = the variance of x across its domain
r = the separation distance
r_o = the covariance distance (a soil parameter).

For the covariance function of Equation 33, the system components become

$$\Psi = e^{-r/r_o} \qquad \text{[Eq 34]}$$

$$E[w^2(t)] = Q = \sigma_x^2(1 - \Psi^2) \qquad \text{[Eq 35]}$$

$$E[x(0)] = 0, \quad E[x^2(0)] = P_o = \sigma_x^2 \qquad \text{[Eq 36]}$$

$$E[v^2(t)] = R = \text{constant}. \qquad \text{[Eq 37]}$$

Table 2 is a summary of seven simulated cases. Case 3 is designated the base case because its covariance distance is that used for the depth-of-cut model in later sections. The other cases show sensitivity of filter estimates to covariance distance r_o, observation variance R, and variance of the state σ_x^2. The last column (designated P_∞) is the estimation variance, $P(t/t)$, for large time. P_∞ is a measure of the limiting precision of the estimate. Figures 4 through 10 show estimated vs. true values of x and time plots of those values.

Figures 4 through 6 show sensitivity with respect to the covariance distance, and as a result the perturbation variance Q; i.e., as the covariance distance (r_o) increases, the estimates increase in accuracy (P_∞ decreases). This is caused by the higher signal-to-noise ratio (P_o/Q) as Q decreases. In the limiting case $r_o \to \infty$ and the process becomes a random constant with $P_\infty \to 0$ (after a large number of observations the constant is exactly estimated).

As expected, cases 3, 4, and 5 show that an increase in observation variance, R, increases the uncertainty in the estimate of x. Cases 6 and 7 demonstrate the analogous result that an increase in the fluctuation of x ($P_o = \sigma_x^2$) decreases the accuracy of the estimate. The implications of these mathematical properties for blade control are consistent with the intuitive notions that (1) the less precisely blade force are measured, the less precisely depth of cut can be estimated, and (2) the more variable soil properties are, the less precisely depth of cut can be estimated. The behavior of the asymptotic estimator variance P_∞ indicates the performance properties of the estimator when the COV has plowed a long way (i.e., when initial effects have been attenuated).

6 ESTIMATING DEPTH OF CUT FROM BLADE LOAD

This chapter presents results of simulation studies to assess the feasibility of estimating the depth of cut from measured blade force. The problem is modeled as a stochastic control (estimation) problem, where the state variables are depth of cut and undrained shear strength of the soil, and force is a nonlinear response to the state variables.

System Model

The dynamics of depth of cut depend on mechanical characteristics of the blade, the dynamics of control, and the magnitude of noise in the system. The difference equation governing depth of cut is taken as

$$d(t+1) = \Psi_d d(t) + \Gamma u(t) + w_d(t) \qquad \text{[Eq 38]}$$

where $d(t)$ = the (scalar) depth of cut at time t
$u(t)$ = the (scalar) control input
$w_d(t)$ = (scalar) random noise.

Note that Equation 38 implies that the depth of cut, at zero control [$w_d(t) = 0$], follows a one-step Gauss-Markov process.

In reality the dynamics of the blade may differ from the system of Equation 38. However, as long as the state equation can be presented in a linear stochastic difference equation, the details of the estimation process are only slightly changed.

For the present simulation studies, the following parameters were taken as representative.

$$E[d(t)] = 2 \text{ ft}, \qquad E[(d(t) - 2)^2] = P_o = 0.50 \text{ ft}^2$$

$$\Psi_d = e^{-1/\tau_o} = e^{-1/10} = 0.905 \qquad \text{[Eq 39]}$$

$$E[w_d(t)] = 0, \qquad E[w_d^2(t)] = (1 - \Psi_d^2) = P_o = 0.091$$

Note that the chosen parameters indicate that the depth-of-cut process has a mean of 2 ft, covariance distance of 10 ft, and standard deviation of 0.5 ft. The mean (2 ft) is approximately the design specification (target value) for mine plowing, the standard deviation (0.5 ft) is a conservative guess at the uncertainty in initial depth of cut, and the covariance distance (10 ft) is a conservative estimate presuming on erratic topography.

In the simulation study it was assumed that the control signal, $u(t)$ is zero, indicating a fixed setting for the blade. For this case, random variations of blade depth are due to noise and changes in topography. The addition of control terms $u(t)$ is to be part of a second phase of the work reported here.

Soil Model

Several assumptions were made to model the soil. A balance was struck between the reduction of variability with volume and discrete changes in soil type (see Chapter 3) by assuming a coefficient of variation of 10 percent, a covariance distance, r_o, of 50 ft, and an average undrained shear strength of 400 psf.

Linearization of Force Model

The force function which was developed in Chapter 2,

$$F = 0.5\gamma d^2 + 2cd + qd \qquad \text{[Eq 40]}$$

in a nonlinear function of the state variables d = depth of cut and c = undrained soil strength (cohesion). This is the function used to relate observations $\underline{y}(t)$ to the state variables $\underline{x}(t)$. To make the force function linear, it was expanded in a Taylor series about the mean values of d and c and truncated to the first two terms. Denoting the mean values of depth and undrained shear strength by m_d and m_c,

$$F = F(m_d, m_c) + (d - m_d)\frac{\delta F}{\delta d} + (c - m_c)\frac{\delta F}{\delta c} \qquad \text{[Eq 41]}$$

where the partial derivatives are evaluated at m_c and m_d. Choosing $\gamma = 120$ psf, $q = 0$ (no surcharge), and the mean values $m_d = 2$ ft and $m_c = 400$ psf, the specific blade force (lb/unit width) is,

$$F \approx -1840 + 1040d + 4c \qquad \text{[Eq 42]}$$

To assess the magnitude of error in the linearized form, several comparisons were made. Figure 11 shows the comparison for c = 400 psf, the average soil strength. The approximation is good for depths in the range 1 to 3 ft. Figure 12 is a comparison of estimated vs. true depth in which depth is back-calculated from the linearized force, $d = (F + 240)/1040$. Knowing the true depth, a force is calculated from Equation 5, then the linear approximation is used to back-calculate an approximate depth; then real and approximated depths are compared. The back-calculated depth in Figure 12 is close to the true depth in the range 0.8 to 3 ft.

These comparisons indicate that the error in the linearized force function is small. However, more robust linearization techniques are available if needed.[13]

[13] A. Gelb.

Simulation Case Studies

Based on the above discussion, the following system and observation equations were used to characterize the estimation problems.

$$d(t+1) = \Psi_d d(t) + w_d(t) \qquad \text{[Eq 43]}$$

$$c(t+1) = \Psi_c c(t) + w_c(t) \qquad \text{[Eq 44]}$$

$$F(t) = -1840 + 1040d(t) + 4c(t) + v_F(t) \qquad \text{[Eq 45]}$$

Parameter values are taken from Equations 39 and 42. Equation 45 is the observation of the state parameters through the force model, where a random noise term $v_F(t)$ expresses errors in force measurement (e.g., derived from data such as those in Figure 3).

Three simulation studies were performed on a MicroVAX minicomputer using specially written software. The simulation used (pseudo-) random number generators to obtain values of the noise terms. A sequence of "actual" depths of cut and a sequence of "actual" soil strengths along a presumed plow path were first generated by Equations 43 and 44, respectively. Then, those sequences were used to calculate a sequence of blade forces using Equation 45. The parameters of Equations 43, 44, and 45 were kept the same in each simulation. The sequence of blade forces was "observed" with measurement error (noise) and the "observed" blade forces put through a Kalman filter to simultaneously estimate depth of cut and soil strength at discrete points along the plow path.

Case 1: Perfect Observations

In Case 1 the observations of depth of cut (force) were assumed to be made without errors. The parameters of the noise term in Equation 45 are

$$E[v_F(t)] = 0, \qquad E[v_F^2(t)] = 0 \qquad \text{[Eq 46]}$$

Figure 13 shows the time stream of blade force for the simulated shear strength and blade depth profiles of Figures 14 and 15, respectively. Figures 14 and 15 also show the estimated shear strength and blade depths obtained by applying the Kalman filter of Equation 27 to the time stream of blade force in Figure 13. Scatter plots of estimated and true state variables are shown in Figures 16 and 17.

The accuracy of the estimated depth (Figure 17) was greater than expected. To investigate this finding, force was plotted against depth as shown in Figure 18. The relationship, except for large deviations at around 1.8 to 2.4 ft, is approximately linear, which explains the accuracy of the estimated depth. The reason for this linear behavior is the low coefficient of variation (10 percent) assumed for undrained shear strength ("Soil Model," this chapter). Although c is variable, its variation is small compared to the mean shear strength (400 psf).

The limiting standard deviation of depth-of-cut estimate ($\sqrt{P_\infty}$) in this simulation is 0.075 ft (0.9 in). This suggests that depth of cut might be controlled to within an inch (rms). This standard deviation, however, should be used with caution since this value is calculated for the linearized system.

Case 2: Noisy Observations of Blade Depth

Case 2 was designed to assess the sensitivity of estimates to noise in the force measurement. Two simulations were performed, with the noise in the force model characterized as

$$E[v_F(t)] = 0, \qquad E[v_F^2(t)] = 40000, \qquad \text{[Eq 47]}$$

and

$$E[v_F(t)] = 0, \qquad E[v_F^2(t)] = 160000. \qquad \text{[Eq 48]}$$

Case 2a. In this simulation the variance of the white noise in Equation 45 corresponds, approximately, to a 10 percent coefficient of variation in the force at mean values of the state variables (d = 2 ft and c = 400 psf).

Figure 19 shows the time stream of blade force for the simulated shear strength and depth processes in Figures 20 and 21, which are the same as for case 1.

Figures 22 and 23 compare the Kalman filter estimates of state variables to true values. As expected, the estimates in case 2 are less accurate than case 1, since errors in the force measurement are translated into estimation errors of the state variables.

The limiting standard deviation of depth-of-cut estimate in this simulation is 0.16 ft, about twice as large as in case 1.

Case 2b. The coefficient of variation in the force model in this simulation (Equation 48) is approximately 20 percent at mean values of the state parameters. This value is the same as that calculated from experimental results in Figure 3.

Figure 24 shows the time stream of blade force for the simulated shear strength and depth processes shown in Figures 25 and 26. Note that the true states in this simulation [c(t) and d(t)] are identical to those in case 2a and for case 1.

Figures 27 and 28 compare the Kalman filter estimates of state variables to true values. The estimates are less accurate than simulation 2a, with the shear strength estimate particularly biased. The bias is a combined result of the linearization and the large noise variance.

Case 3: Redundant Observations

The characteristics of the force measurement in case 3 were assumed identical to those in simulation 2b; however, it was assumed that a second, independent, but noisy estimate of depth could be made. The second measurement was modeled as

$$y(t) = d(t) + v_y(t) \qquad \text{[Eq 49]}$$

with noise parameters

$$E[v_y(t)] = 0, \qquad E[v_y^2(t)] = v^2 \qquad \text{[Eq 50]}$$

This provides a two-dimensional vector of measurements.

To assess the improvements in the accuracy of depth estimate as a result of the redundant observation, six simulations were performed for different values of the error variance, v^2, in Equation 50. Table 3 summarizes the results of the simulation. In the table, $(\sqrt{P_\infty})_t^-$ is the limiting standard deviation in case 2b, and $(\sqrt{P_\infty})_t^+$ is the limiting standard deviation with redundant observations. The last column in the table, designated $(\sqrt{P_\infty})_e^+$, is an estimate of $(\sqrt{P_\infty})_t^+$ obtained as

$$(\sqrt{P_\infty})_e^+ = \frac{1}{1/v^2 + (1/P_\infty)^-} \qquad \text{[Eq 51]}$$

The implicit assumption in Equation 51 is that depth of cut is an independent process ($r_o = 0$). The estimate, however, is an upper limit for the correlated process that depth of cut is in reality.

Figure 29 compares $(\sqrt{P_\infty})_t^+$ to $(\sqrt{P_\infty})_e^+$ for values of v in Equation 50. The comparison is close, with a maximum 6 percent deviation. The implication of these results is that redundant measurements of blade depth, even if noisy, substantially improve the precision with which depth of cut can be estimated.

7 CONCLUSIONS

The principal conclusion of this study is that the depth of cut for the COV blade can be estimated with reasonable accuracy from measured blade forces. This means that blade force measurement may provide a satisfactory approach to automating blade control.

In the accepted equation for blade force, if undrained conditions (i.e., rapid shearing) and a smooth blade are assumed, the term for undrained shear strength of the soil being plowed dominates the calculation of blade force. Therefore, the effect of variations in soil unit weight can be and generally are neglected in calculating variations in blade force. The spatial variation of undrained shear strength has been found empirically to be well-modeled by stationary, Gaussian processes with an exponential convariance function. Thus, soil strengths and resulting blade loads are modeled as a Gauss-Markov process. Optimal control theory was used to develop a control equation incorporating random variations in topography and measurement errors, which could be used to control blade depth on the COV. This control equation requires estimates of depth of cut, obtained using a Kalman filter. Simulation studies indicate that as covariance distances in soil properties and topographic variations increase, the precision of estimates of blade depth increases. Similarly, as the variance of observation errors increases, the precision of blade depth estimates decreases.

The simulation studies were based on a linearized form of the blade force equation which was adopted to simplify the control equations. The error introduced by the linearization was found to be small. Parameter values for the simulations were selected to conform to operation specifications for the COV and to empirically typical soil properties. When measurements were assumed to be error free, the standard error of the estimate of depth of cut was found to be as low as 0.9 in., much smaller than expected. When measurement noise was increased to a 10 percent coefficient of variation (i.e., 10 percent of the force), the standard error in the estimate of depth of cut rose to 1.9 in., still considered modest. Further increases in measurement noise led to further increases in the standard error of the depth of cut estimate.

Simulation experiments were also undertaken presuming that a second, independent measurement of blade cut could be made in conjunction with blade force. Significant increases in estimate precision (i.e., decreases in standard error) can be realized using such a redundant measurement, even if the noise in that second measurement is large.

While direct force measurement appears a fruitful approach to controlling blade depth, increased precision can be gained by using one or more redundant sensor systems. These redundant systems need not be highly accurate to be effective.

METRIC CONVERSIONS

1 in. = 2.54 cm
1 ft = 0.3048 m
1 psf = 4.882×10^{-4} kg/m^2

REFERENCES

Astrom, K. J., *Introduction to Stochastic Control Theory* (Academic Press, New York, NY, 1970).

Baecher, G. B., M. Chan, T. S. Ingra, T. Lee, and L. R. Nucci, "Geotechnical Reliability of Offshore Gravity Platforms," M.I.T. Sea Grant, Report MITSG 80-20, Cambridge, MA, 1980.

Bryson, A. E., and Y. C. Ho, *Applied Optimal Control* (Blaisdell Publishing Co., Waltham, MA, 1969).

De Groot, D. J., "Maximum Likelihood Estimation of Spatially Correlated Soil Properties," M.S. Thesis, M.I.T., May 1985.

Gelb, A., *Applied Optimal Estimation* (M.I.T. Press, Cambridge, MA, 1974).

Kalman, R. E., "A New Approach to Linear Filtering and Prediction Problems," *American Society of Mechanical Engineers (ASME) Journal of Basic Engineering*, Vol 82 (1960), pp 34-45.

Kalman, R. E., and R. S. Bucy, "New Results in Linear Filtering and Prediction Theory," *ASME Journal of Basic Engineering*, Vol 83 (1961), pp 95-107.

Lambe, T. W., and V. R. Whitman, *Soil Mechanics* (John Wiley & Sons, New York, 1968).

O'Callaghan, J. R., and P. J. McCullen, "Soil Mechanics in Relation to Earth-Moving Machinery," *Institution of Mechanical Engineers—Proceedings* (Symposium on Earth-Moving Machinery), Vol 179, part 3F (1964-65), pp 23-29.

Spikula, D., "Statistical Estimation of Soil Properties: An Application," M.S. Thesis, M.I.T., May 1983.

Tang, W., "Probabilistic Evaluation of Penetration Resistance," *American Society of Civil Engineers Journal, Geotechnical Engineering Division*, Vol 105, GT10 (1979), pp 1173-1191.

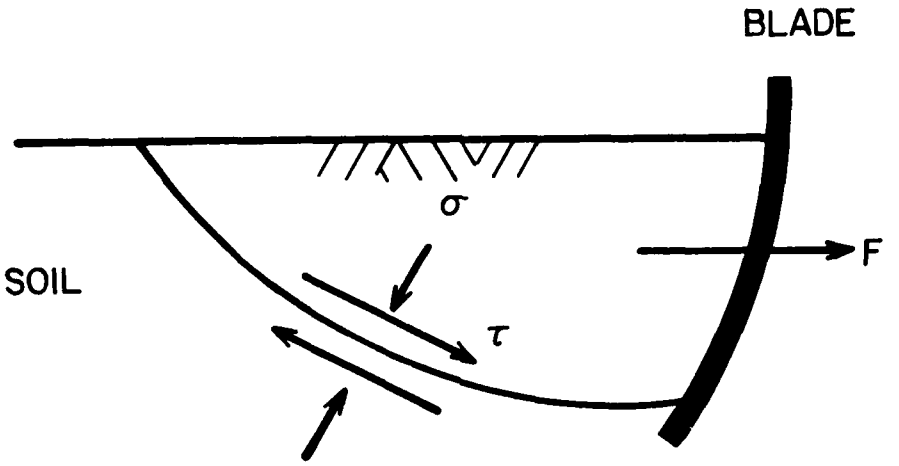

Figure 1. Stresses within the soil mass at failure.

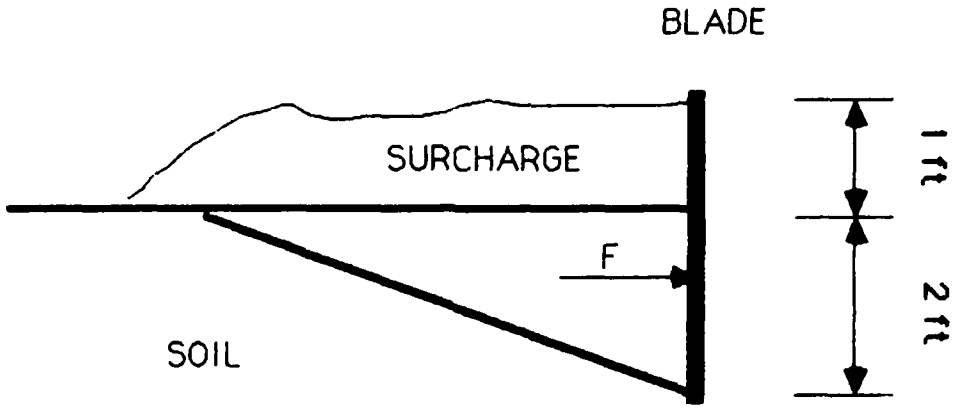

Figure 2. Typical plowing case for the COV.

Table 1

Contribution to Total Force

c/γ	$F = 0.5\gamma d^2$	Lift	2cd Shear	qd Surcharge
2	100%	16.5%	67%	16.5%
3	100	12.5	75	12.5
4	100	10.0	80	10.0
5	100	8.3	83	8.3
6	100	7.0	86	7.0

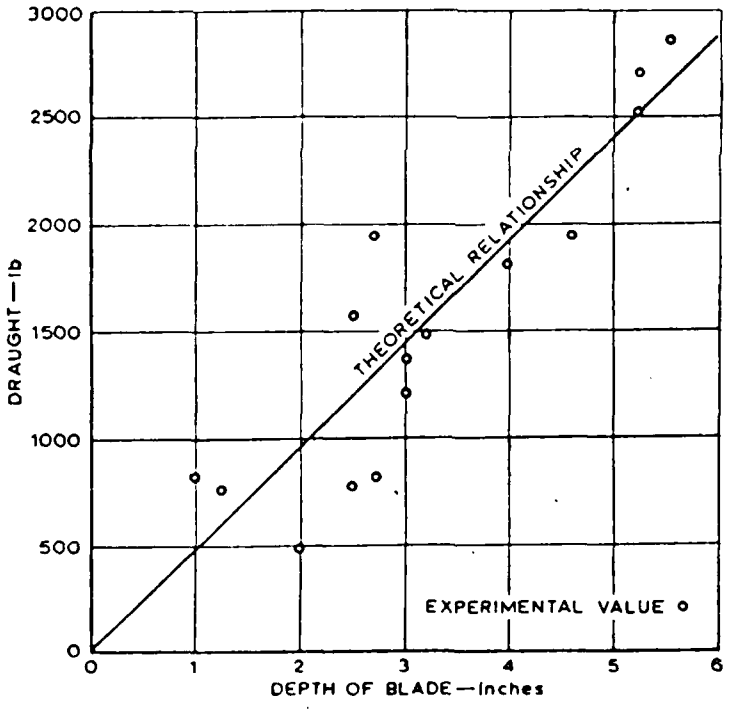

Figure 3. Measured and theoretical values of soil resistance for bulldozer blade. c = 3.8 lb/in./in., φ = 0.0. (Source: J. R. O'Callaghan and P. J. McCullen, "Soil Mechanics in Relation to Earth-Moving Machinery," *Institution of Mechanical Engineers—Proceedings* (Symposium on Earth-Moving Machinery), Vol 179, part 3F (1964-65), pp 23-29.

Table 2

Parameters for Kalman Filter Simulation

CASE	r_o	P_o	R	Ψ	Q	SENSITIVITY	P_∞
1	0.1	0.5	0.5	0.000	0.50	ro	0.69
2	1.0	0.5	0.5	0.368	0.43	ro	0.50
3	10	0.5	0.5	0.905	0.09	BASE	0.39
4	10	0.5	0.1	0.905	0.09	R	0.20
5	10	0.5	1.0	0.905	0.09	R	0.50
6	10	1.0	0.5	0.905	0.18	Po	0.42
7	10	0.1	0.5	0.905	0.02	Po	0.33

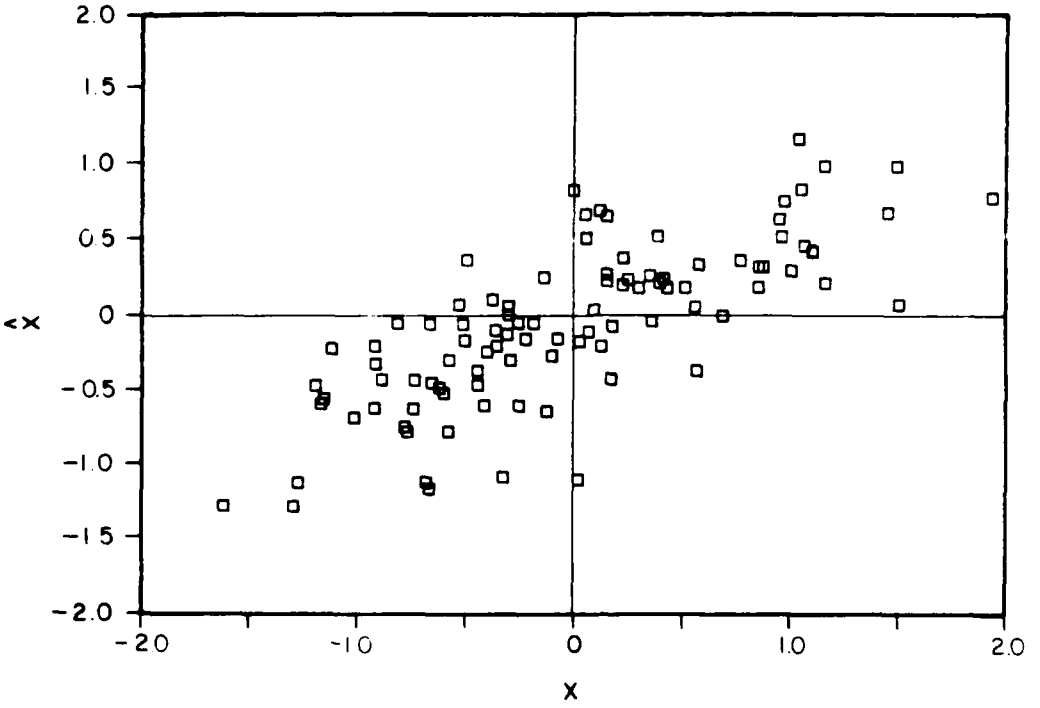

(a)

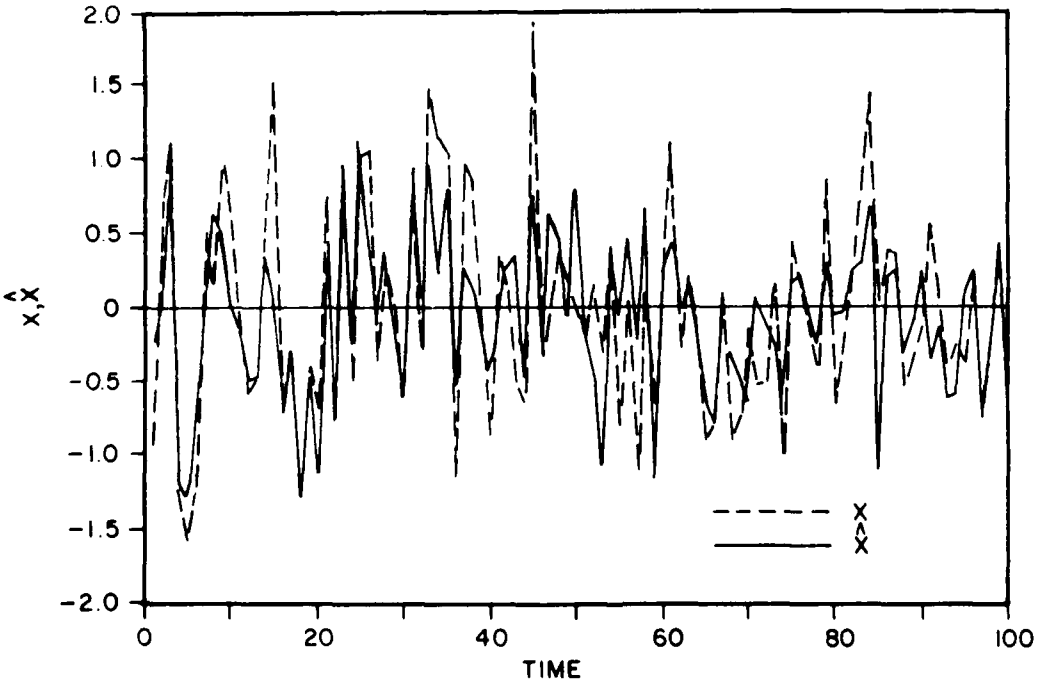

(b)

Figure 4. **(a) Scatter plot and (b) time plot of x and $\hat{x}$ for simulation parameters of case 1 in Table 2.**

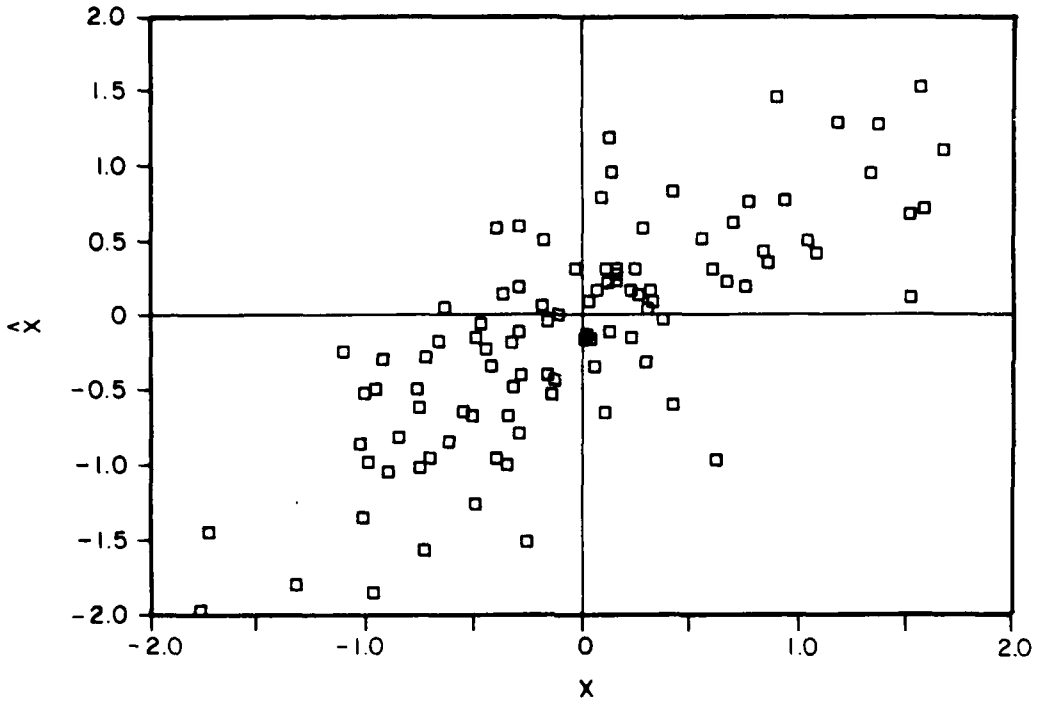

(a)

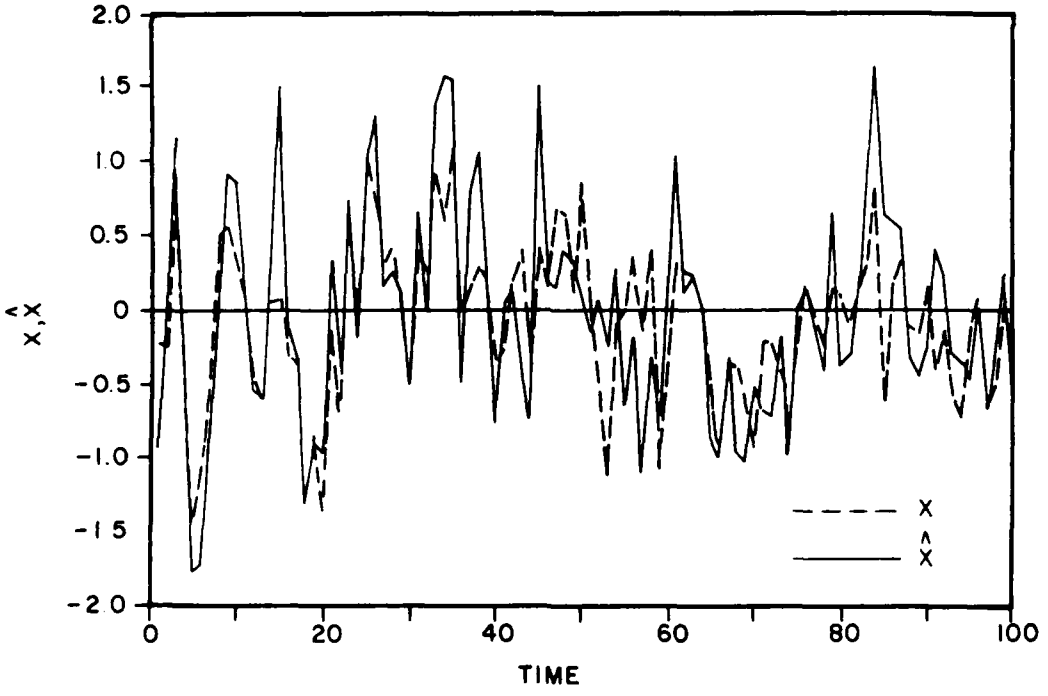

(b)

Figure 5. (a) Scatter plot and (b) time plot of x and $\hat{x}$ for simulation parameters of case 2 in Table 2.

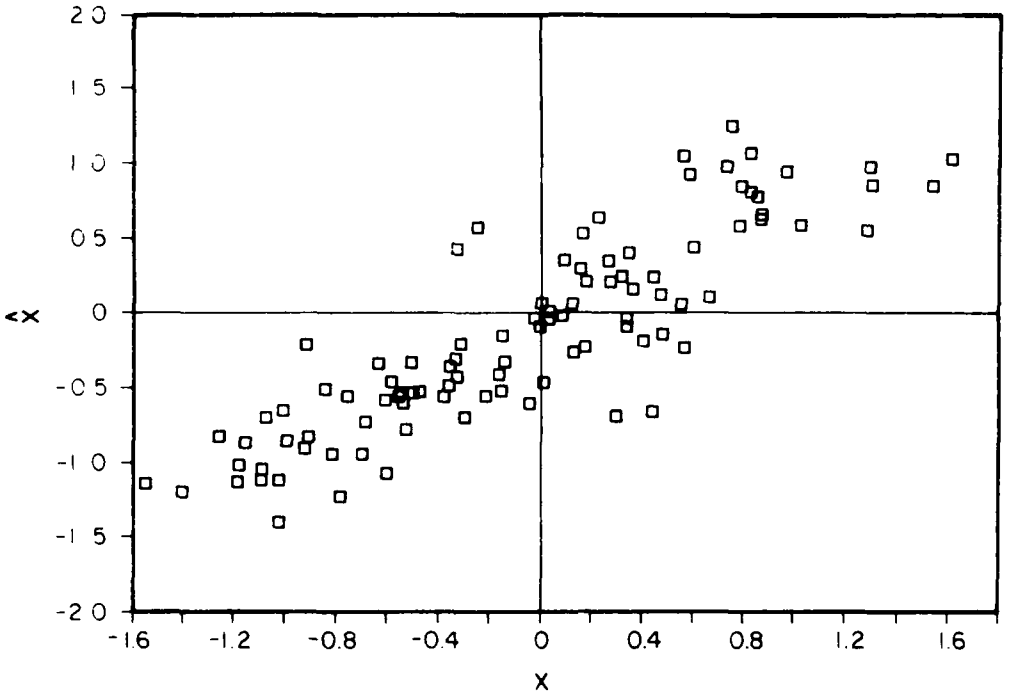

(a)

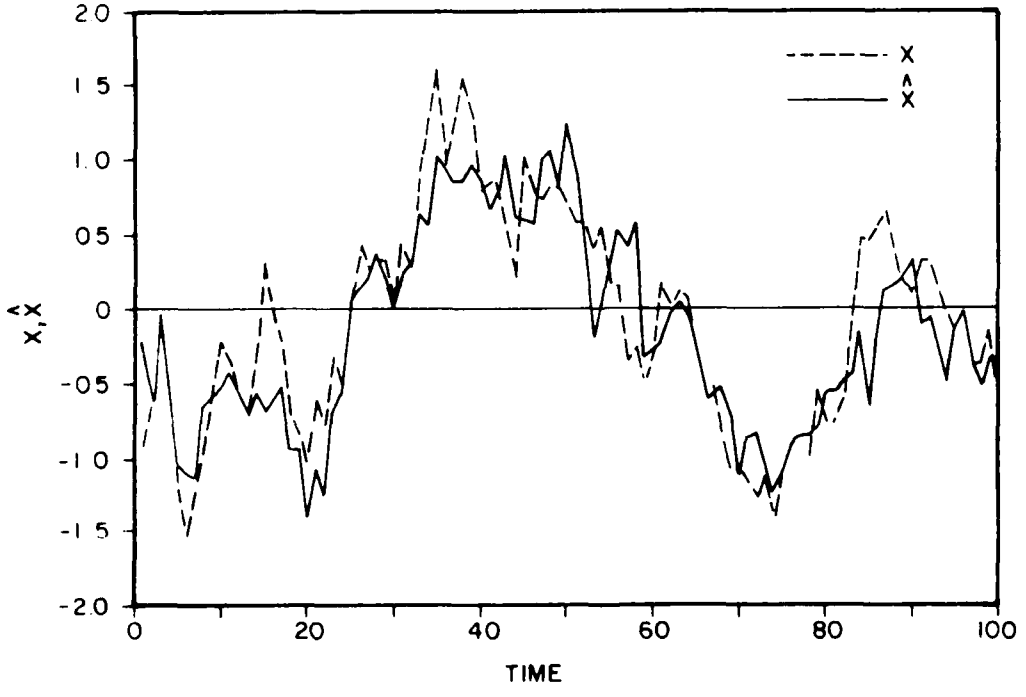

(b)

Figure 6. **(a) Scatter plot and (b) time plot of x and $\hat{x}$ for simulation parameters of case 3 in Table 2.**

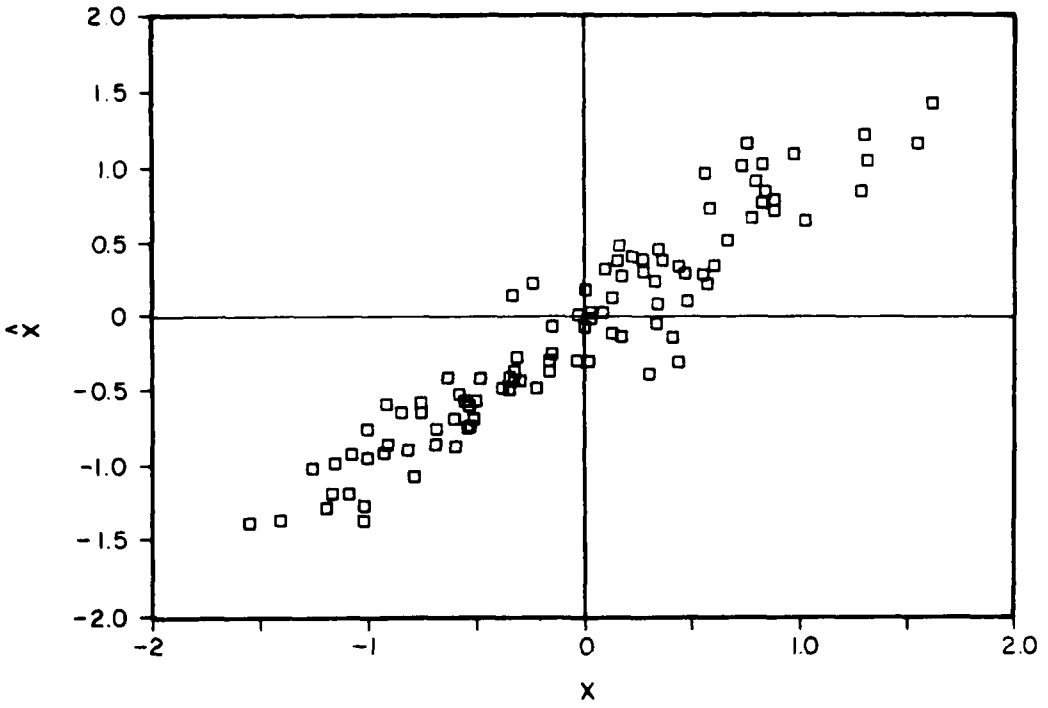

(a)

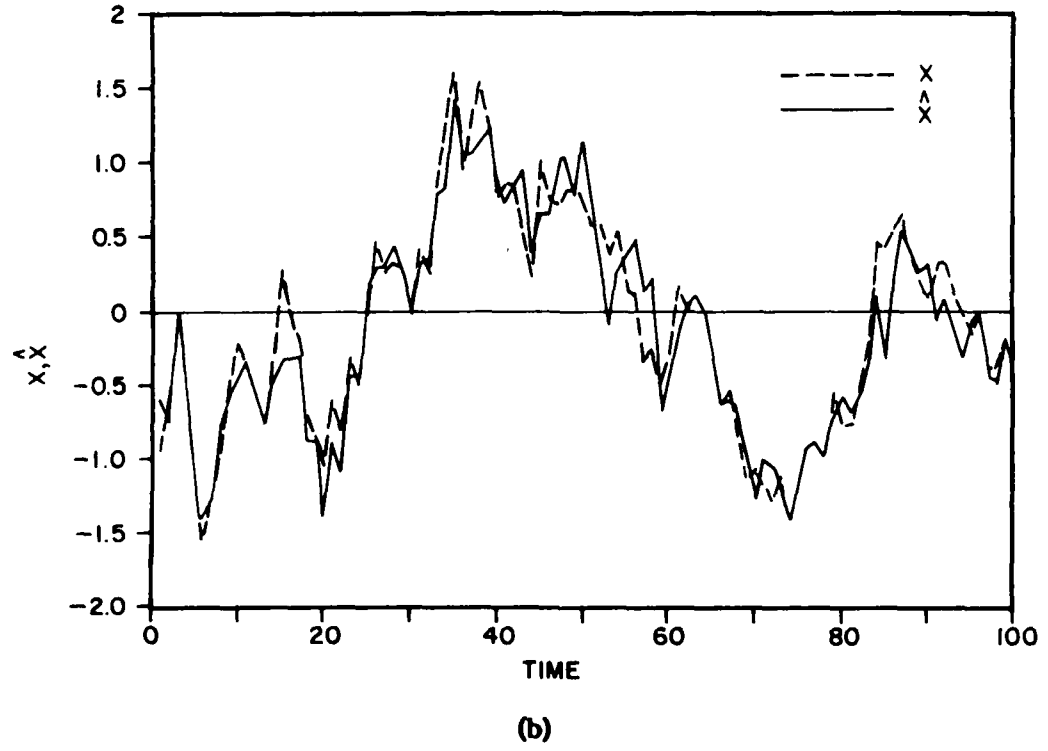

(b)

Figure 7. (a) Scatter plot and (b) time plot of x and $\hat{x}$ for simulation parameters of case 4 in Table 2.

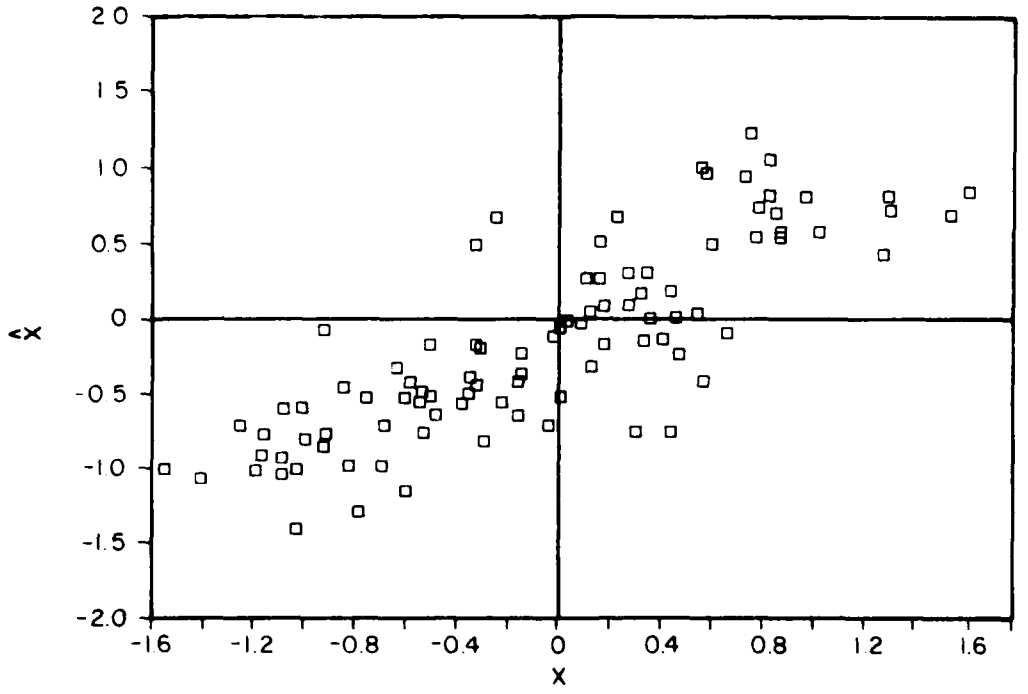

(a)

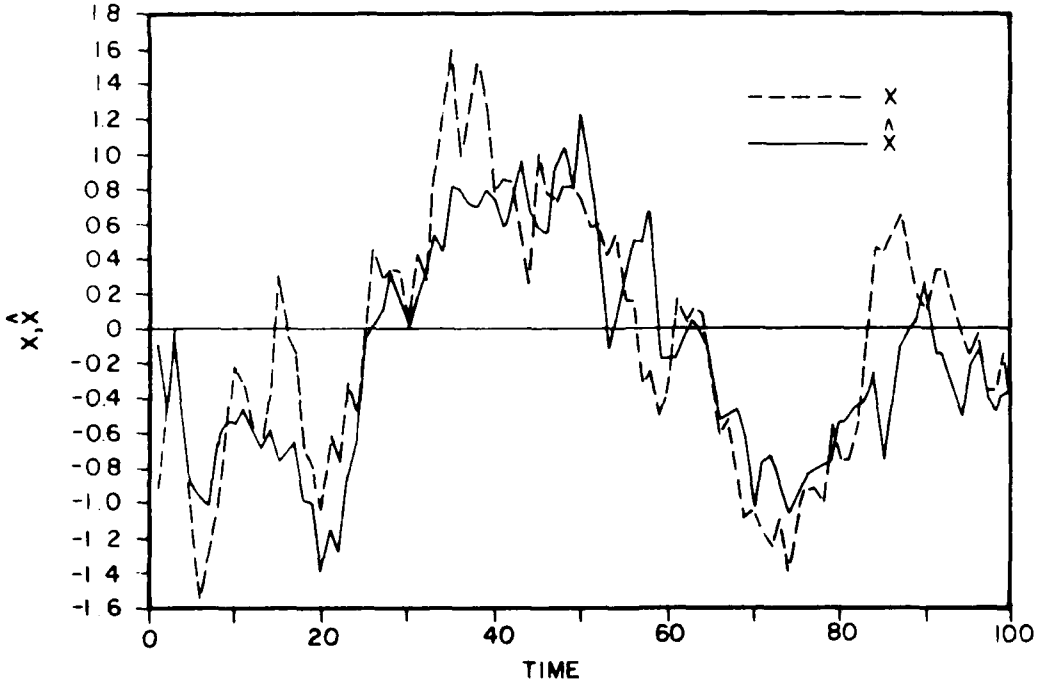

(b)

Figure 8. **(a) Scatter plot and (b) time plot of x and $\hat{x}$ for simulation parameters of case 5 in Table 2.**

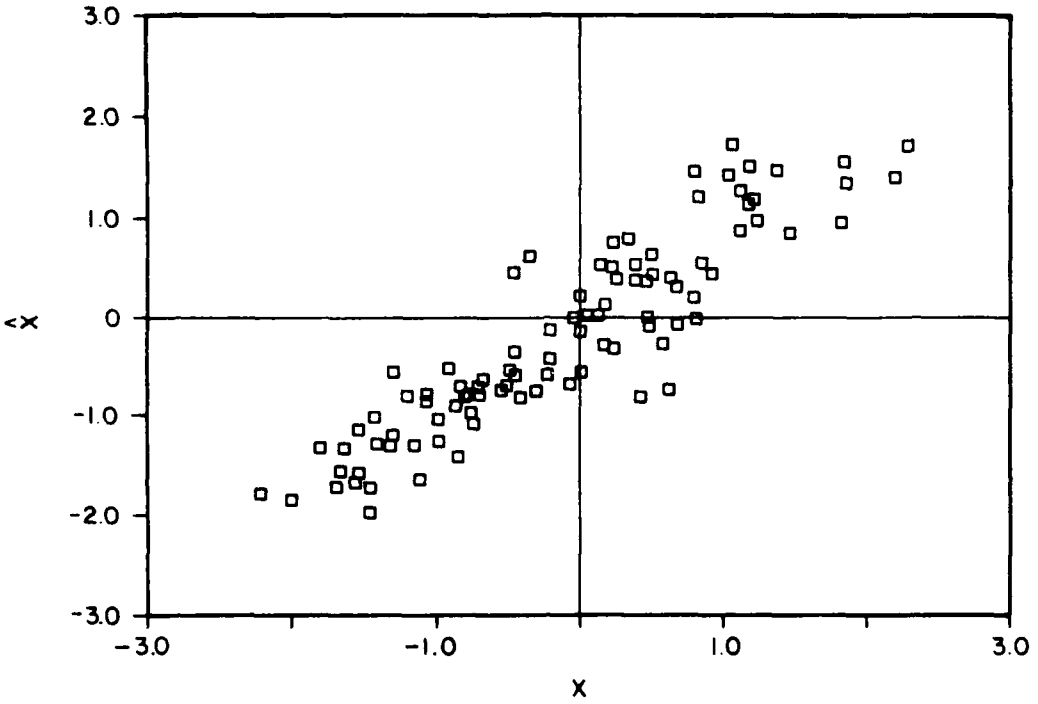

(a)

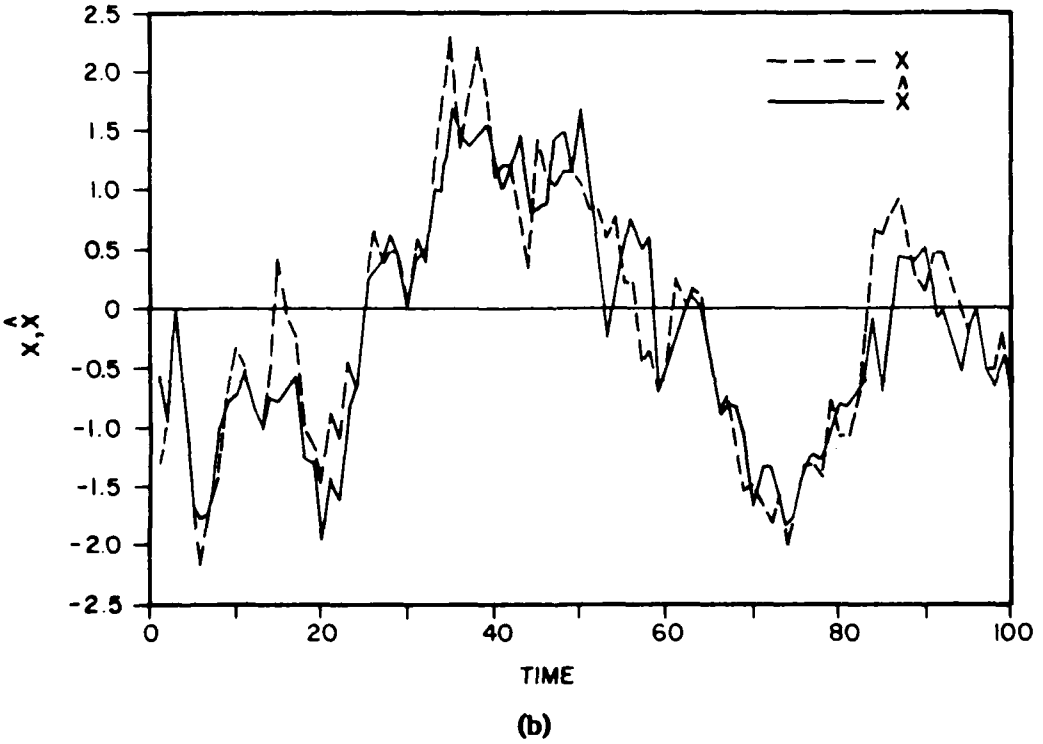

(b)

Figure 9. (a) Scatter plot and (b) time plot of x and $\hat{x}$ for simulation parameters of case 6 in Table 2.

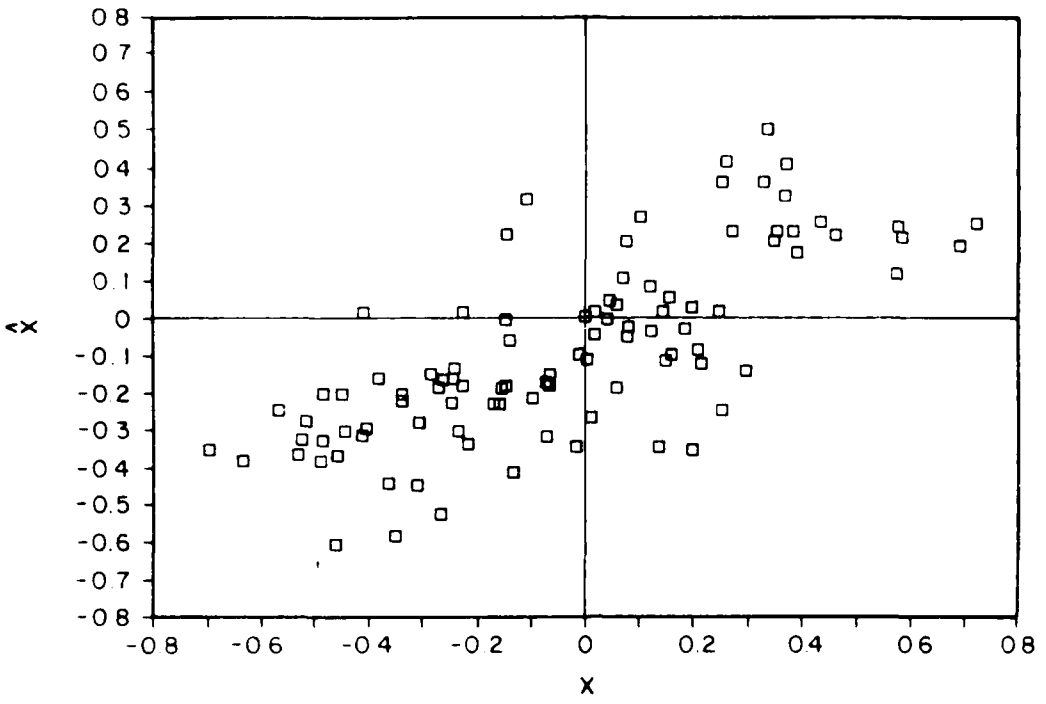

(a)

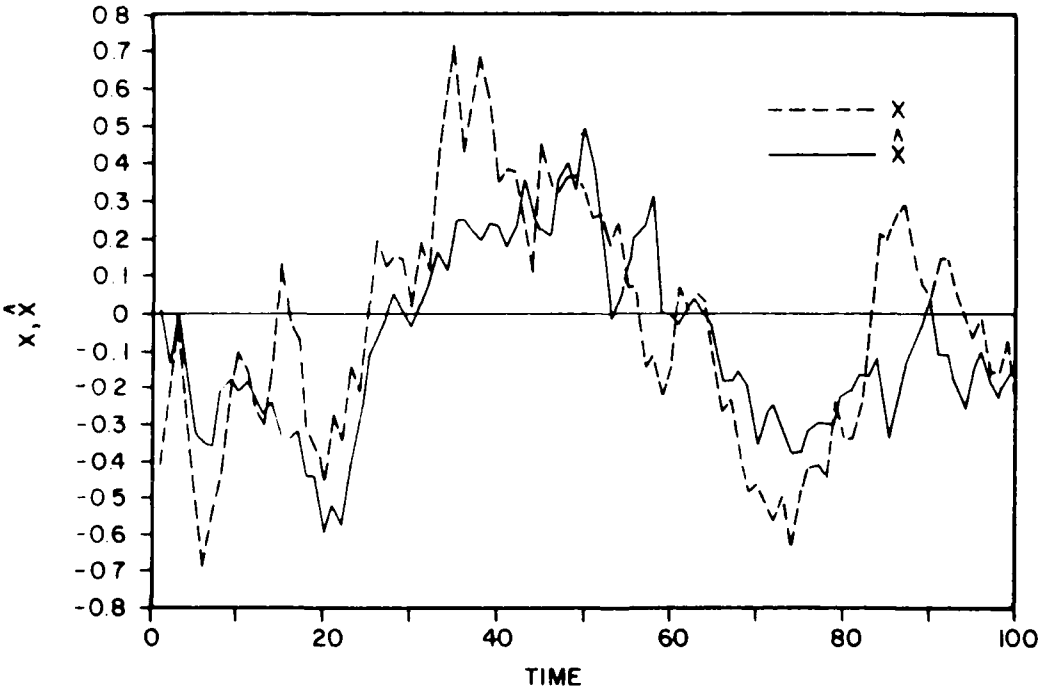

(b)

Figure 10. (a) Scatter plot and (b) time plot of x and $\hat{x}$ for simulation parameters of case 7 in Table 2.

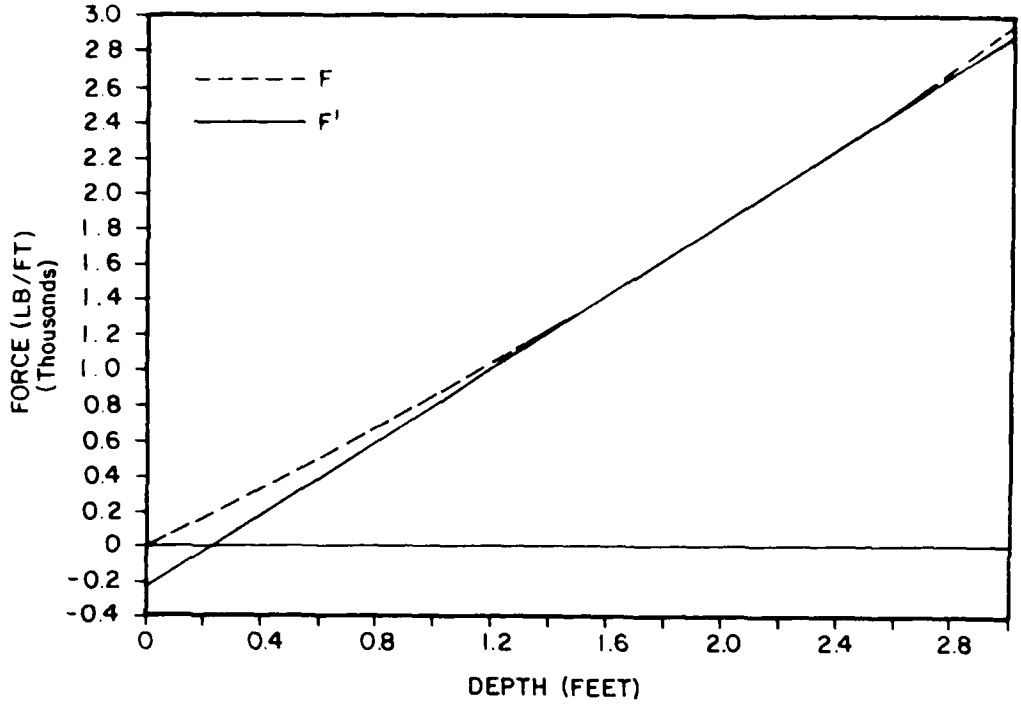

Figure 11. True force F vs. linearized force F' for d = 2 ft and c = 400 psf.

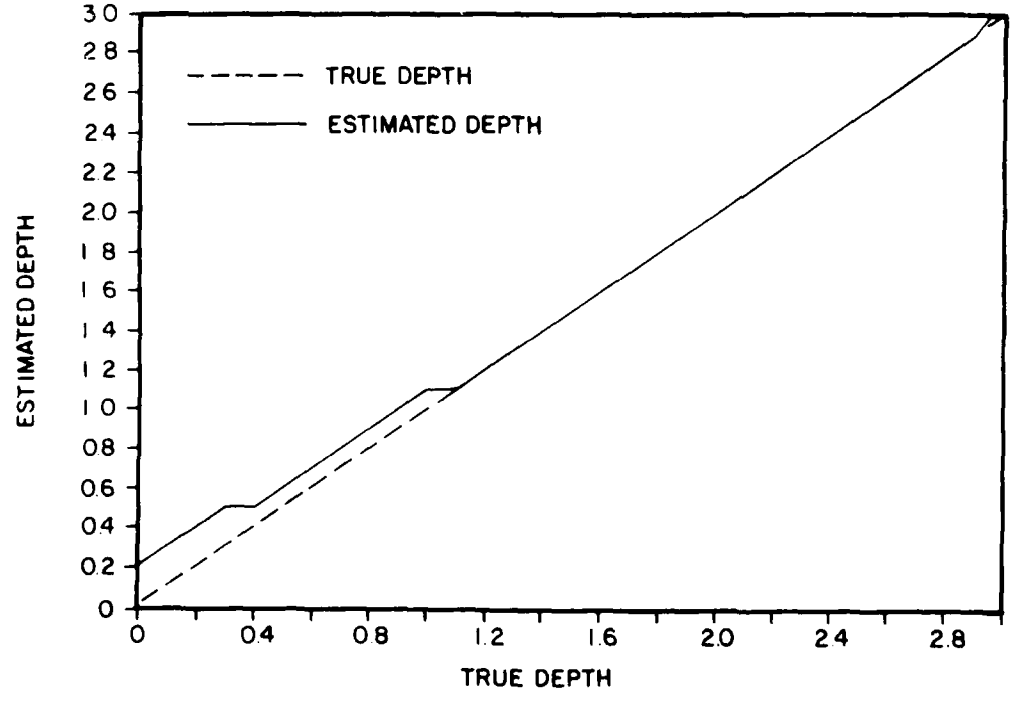

Figure 12. Back-calculated depth (in feet) from linearized force for c = 400 psf.

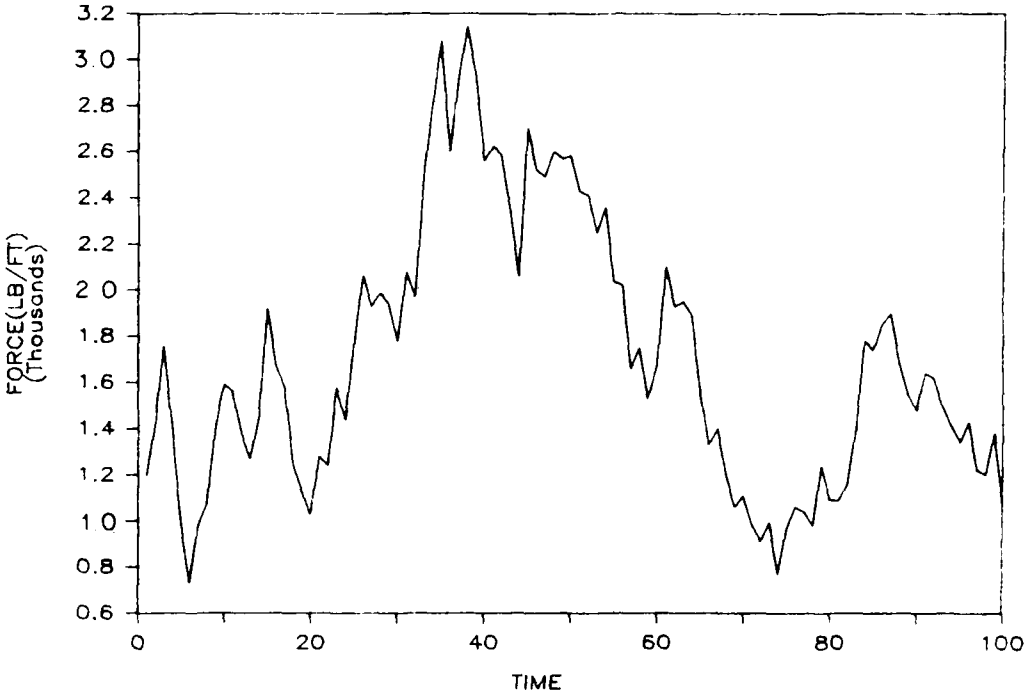

Figure 13. Time plot of force for case 1.

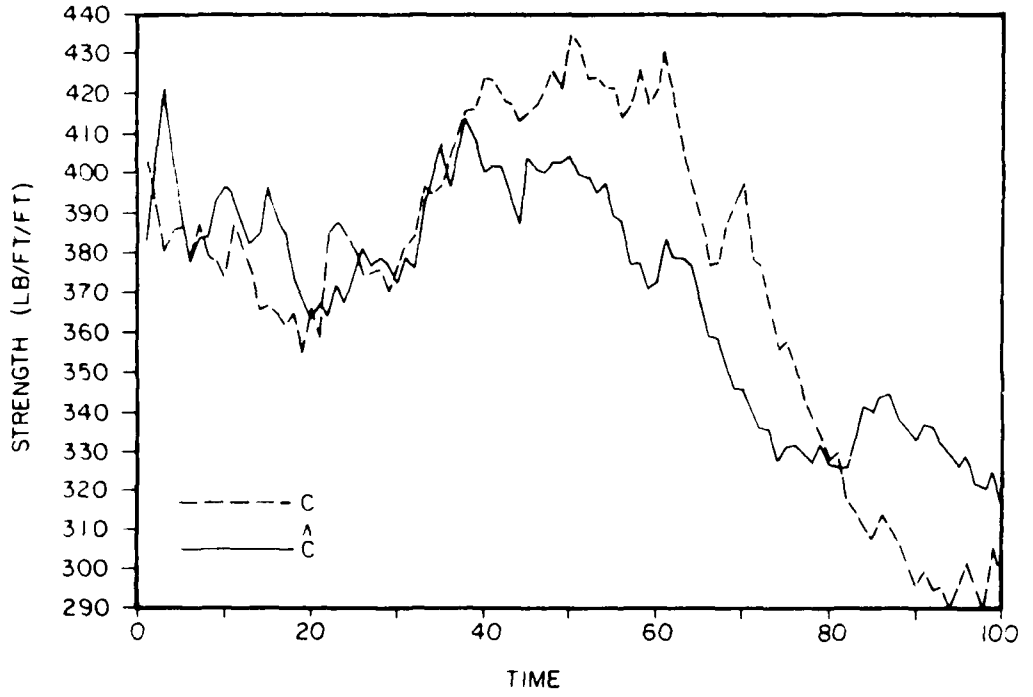

Figure 14. Time plot of true shear strength c and estimated shear strength $\hat{c}$ for case 1.

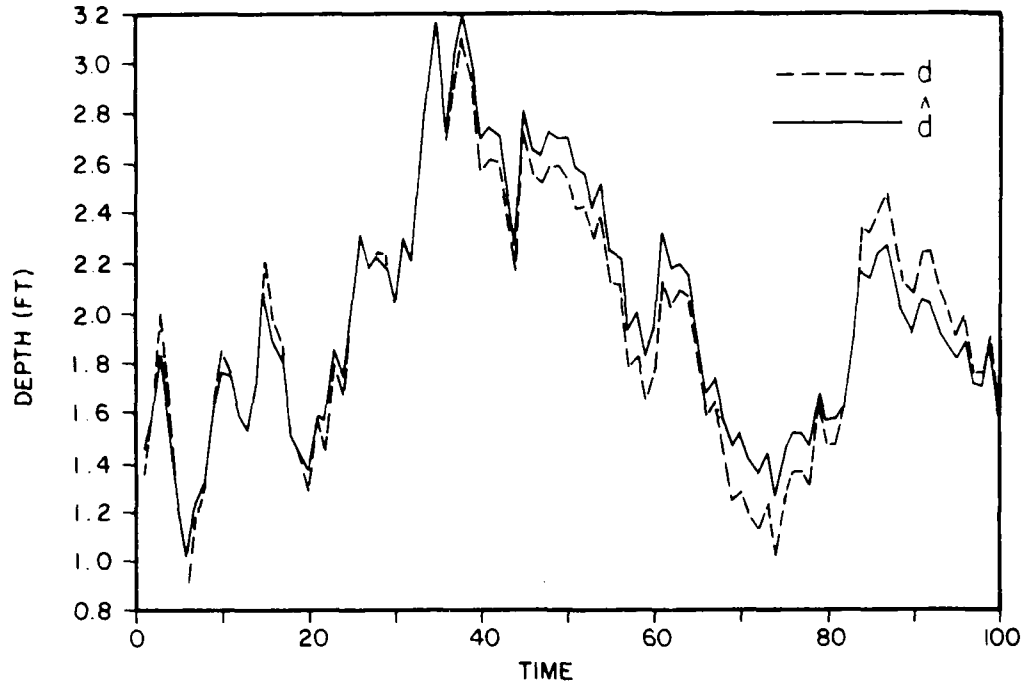

Figure 15. Time plot of true depth d and estimated depth $\hat{d}$ for case 1.

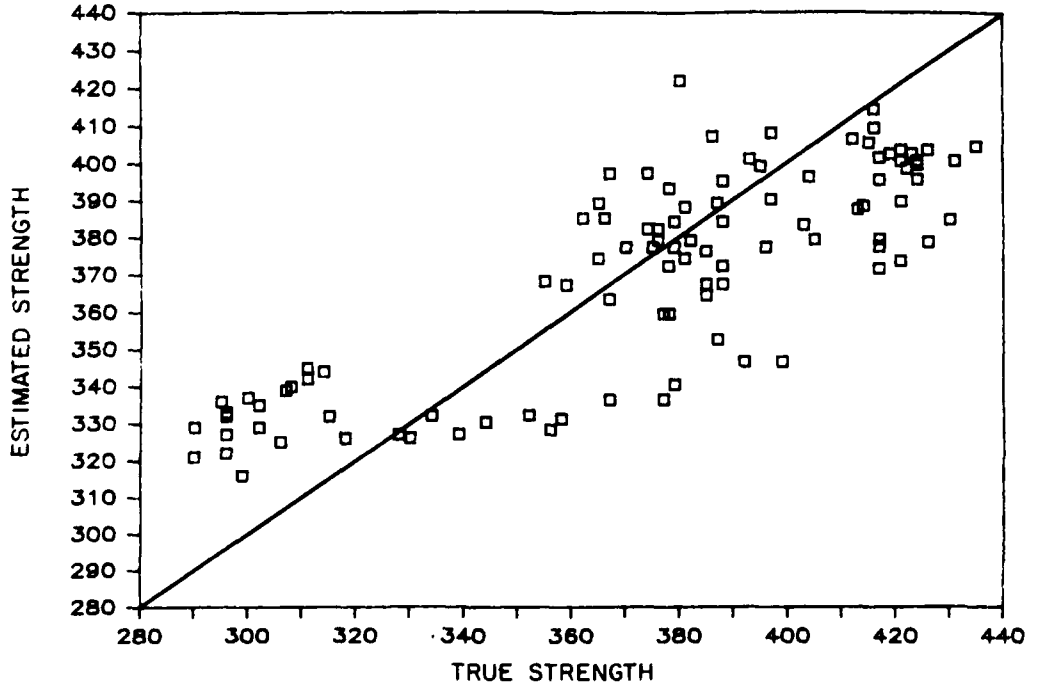

Figure 16. Estimated vs. true shear strength for case 1.

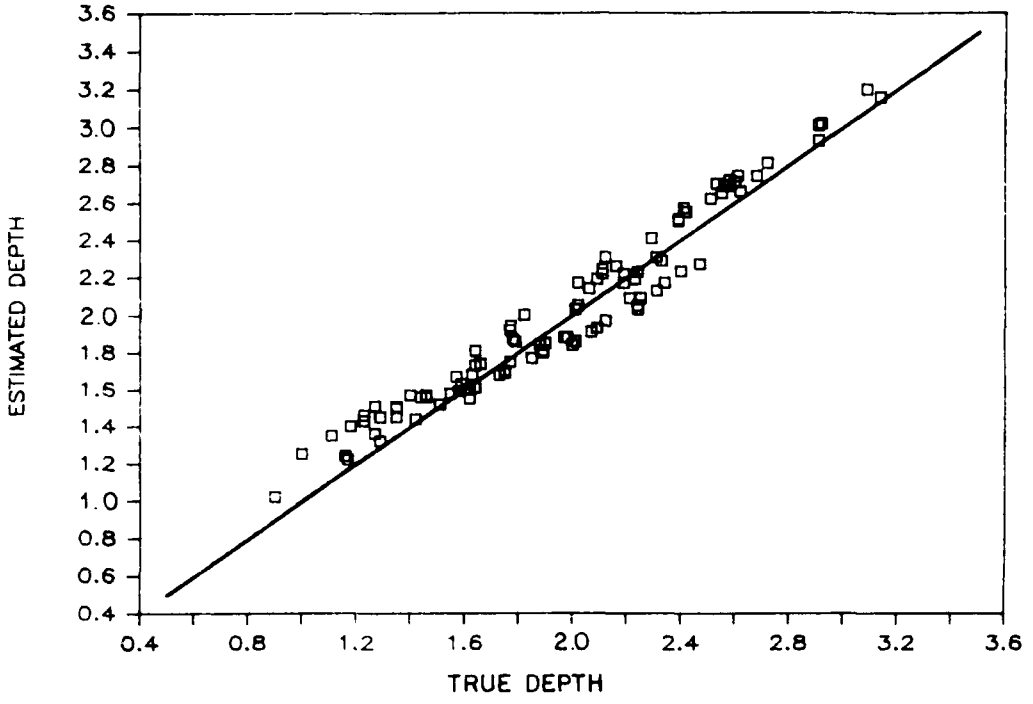

Figure 17. Estimated vs. true depth for case 1.

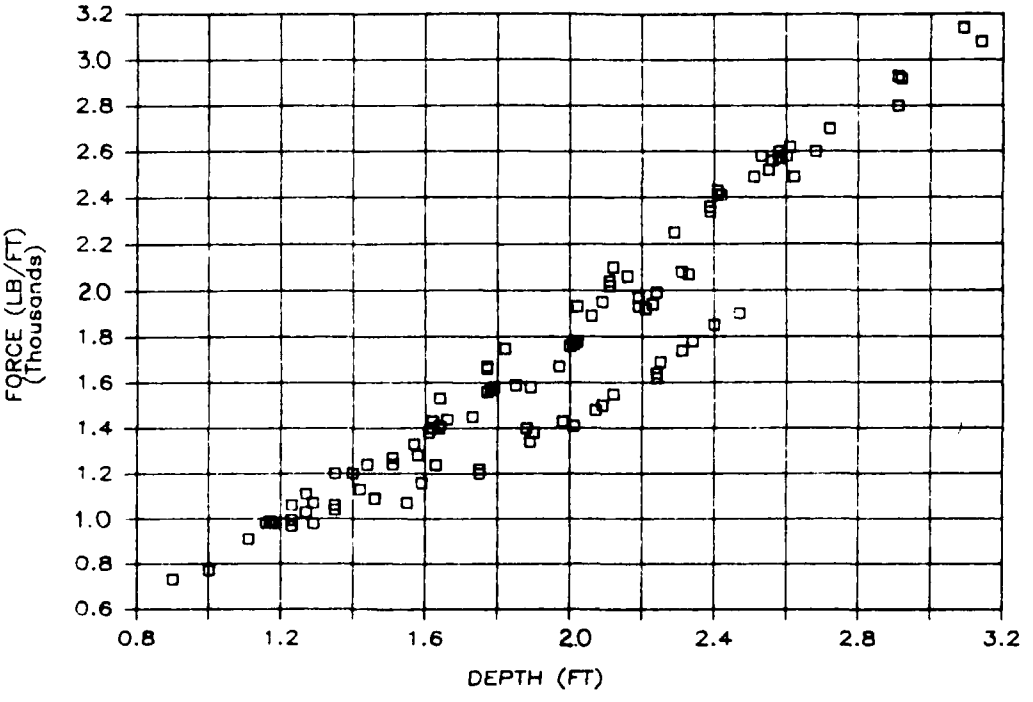

Figure 18. Plot of force vs. true depth of cut for case 1.

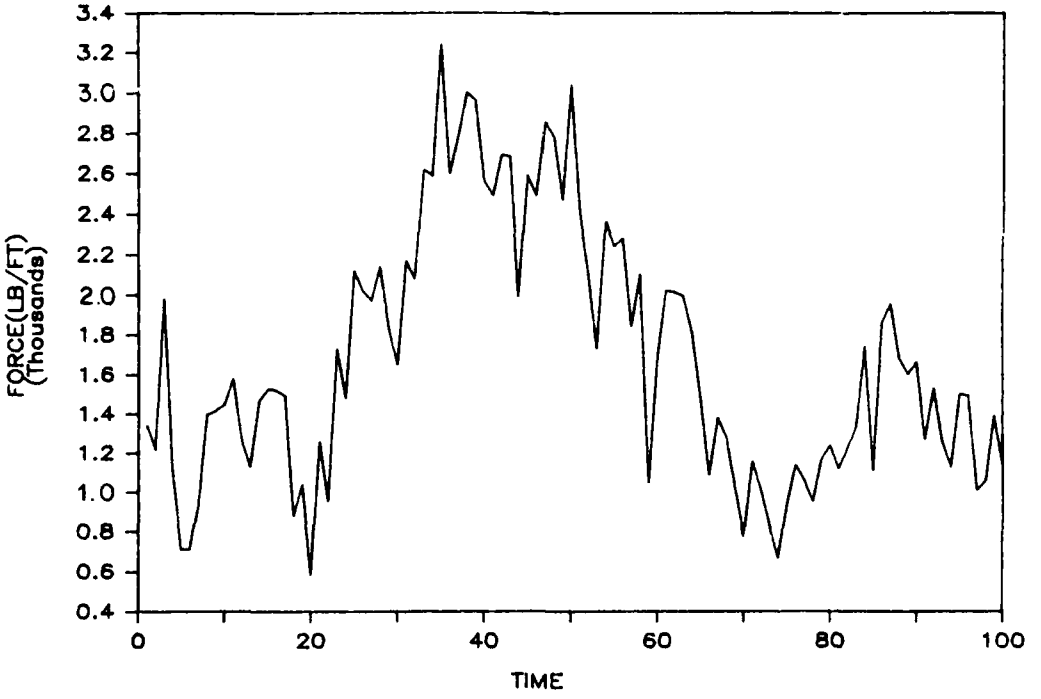

Figure 19. Time plot of force for case 2a.

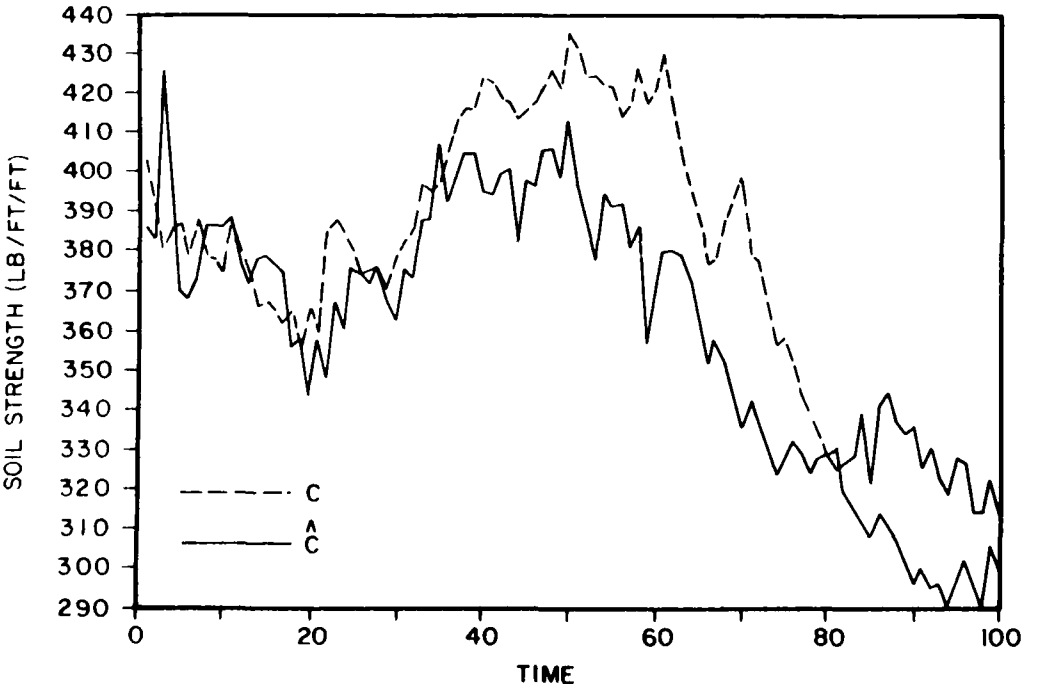

Figure 20. Time plot of true shear strength c and estimated shear strength $\hat{c}$ for case 2a.

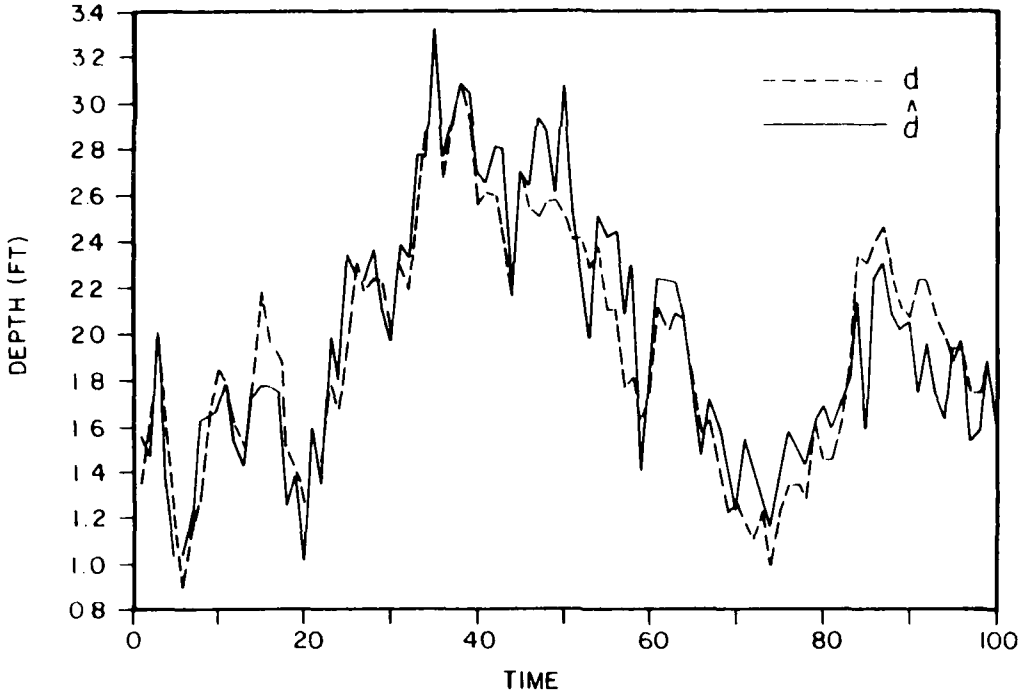

Figure 21. Time plot of true depth d and estimated depth $\hat{d}$ for case 2a.

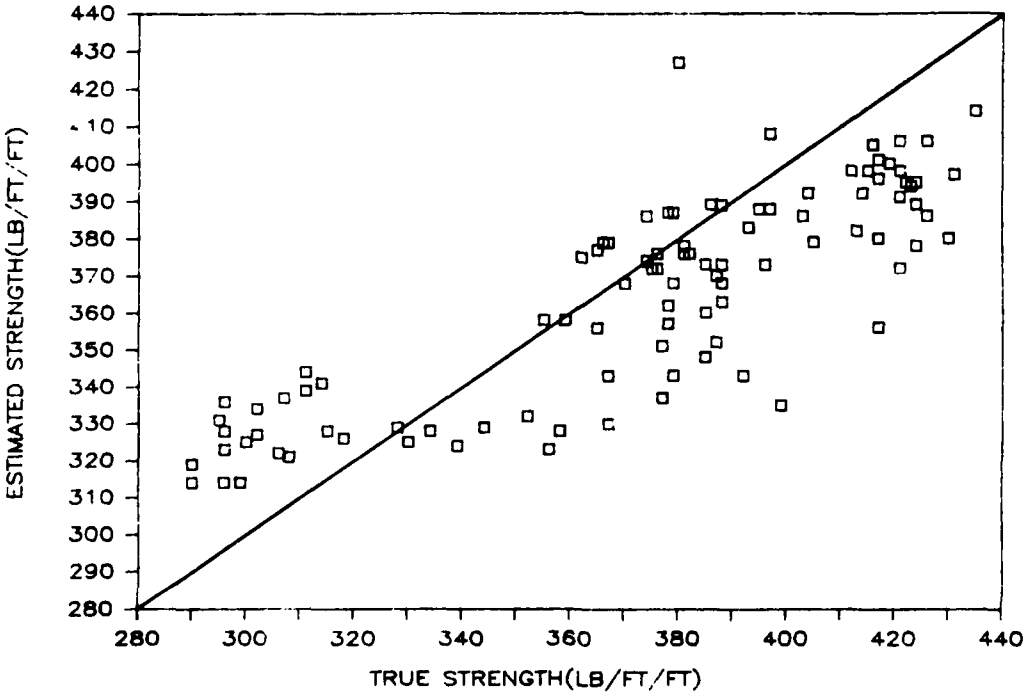

Figure 22. Estimated vs. true shear strength for case 2a.

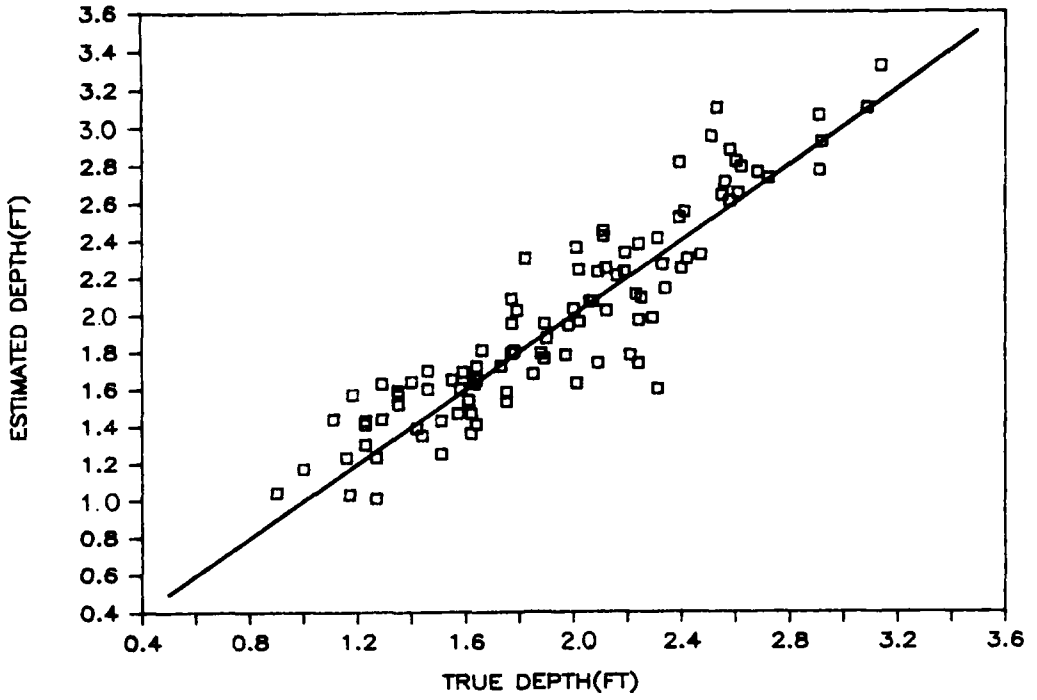

Figure 23. Estimated vs. true depth for case 2a.

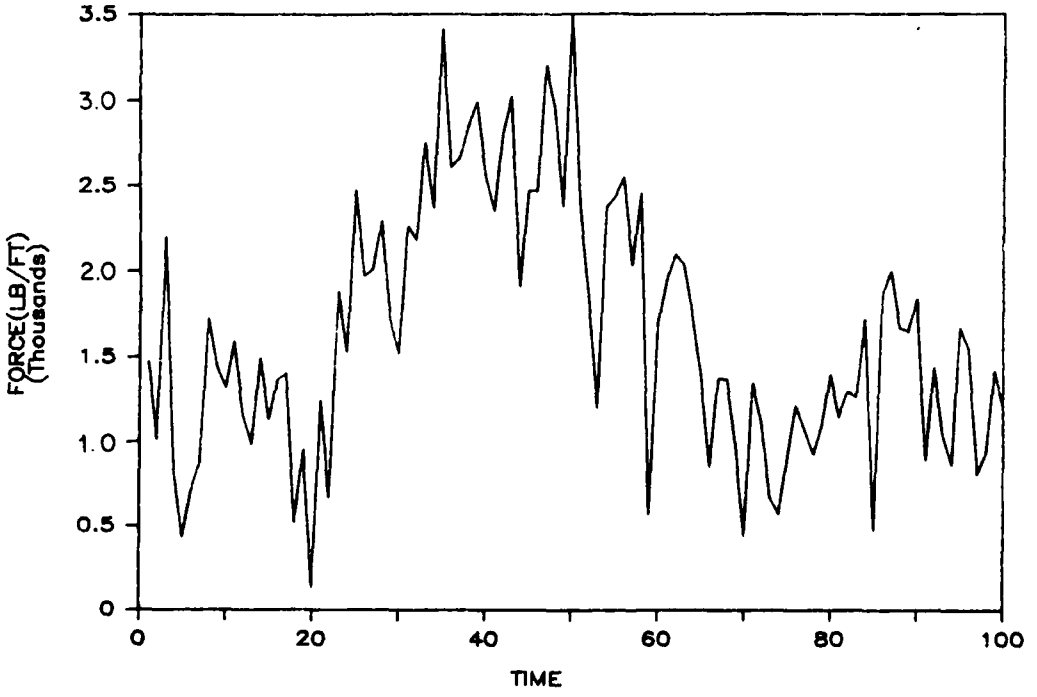

Figure 24. Time plot of force for case 2b.

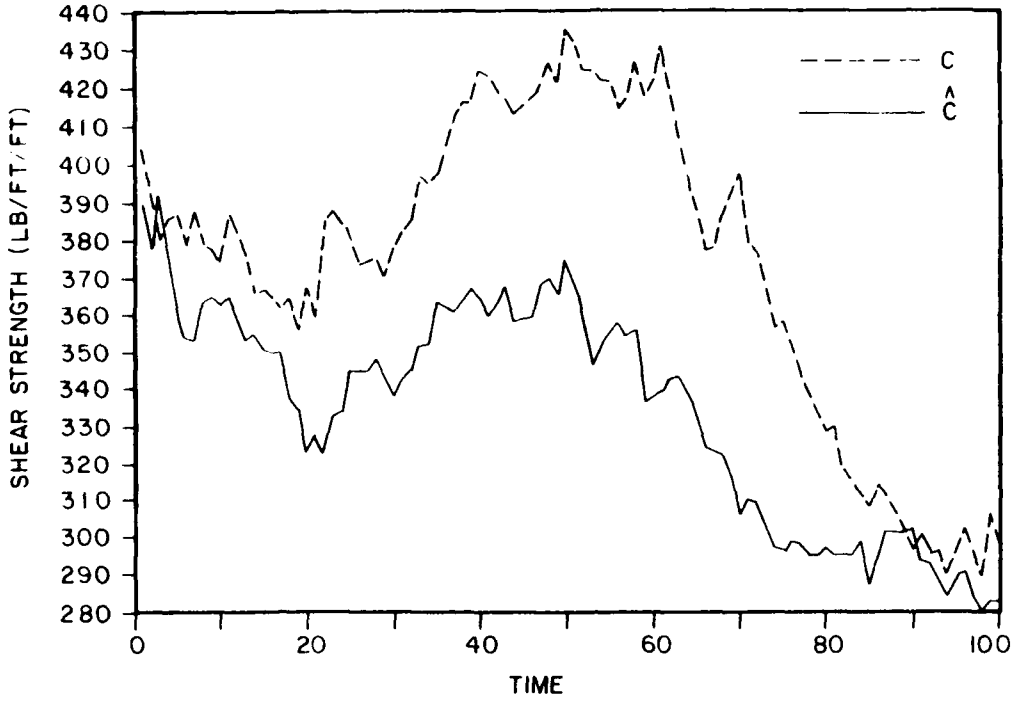

Figure 25. Time plot of true shear strength c and estimated shear strength $\hat{c}$ for case 2b.

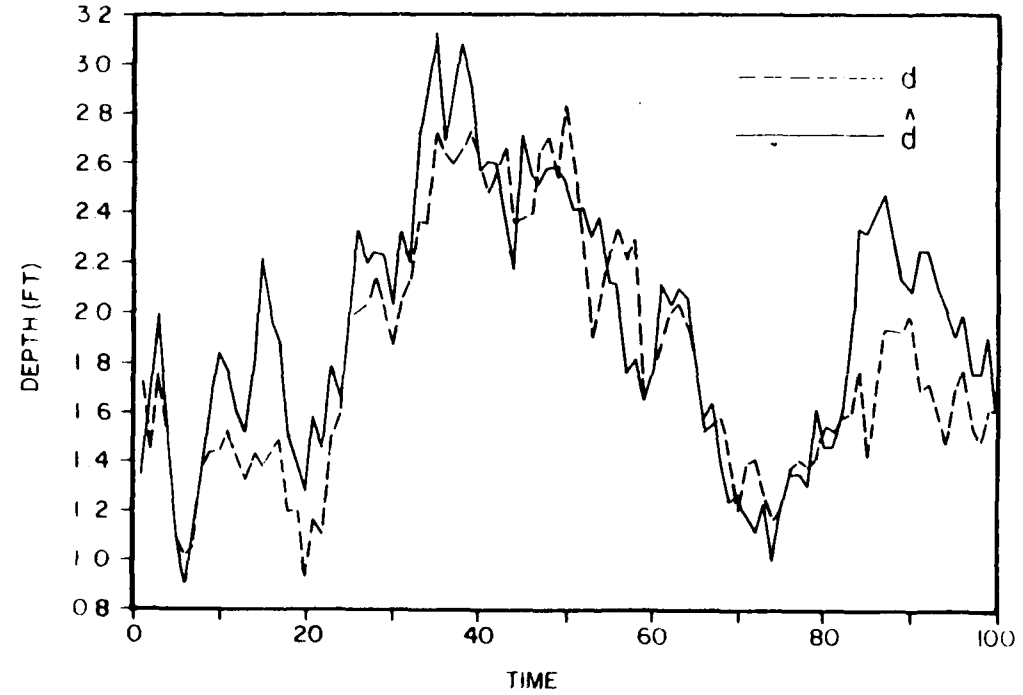

Figure 26. Time plot of true depth d and estimated depth $\hat{d}$ for case 2b.

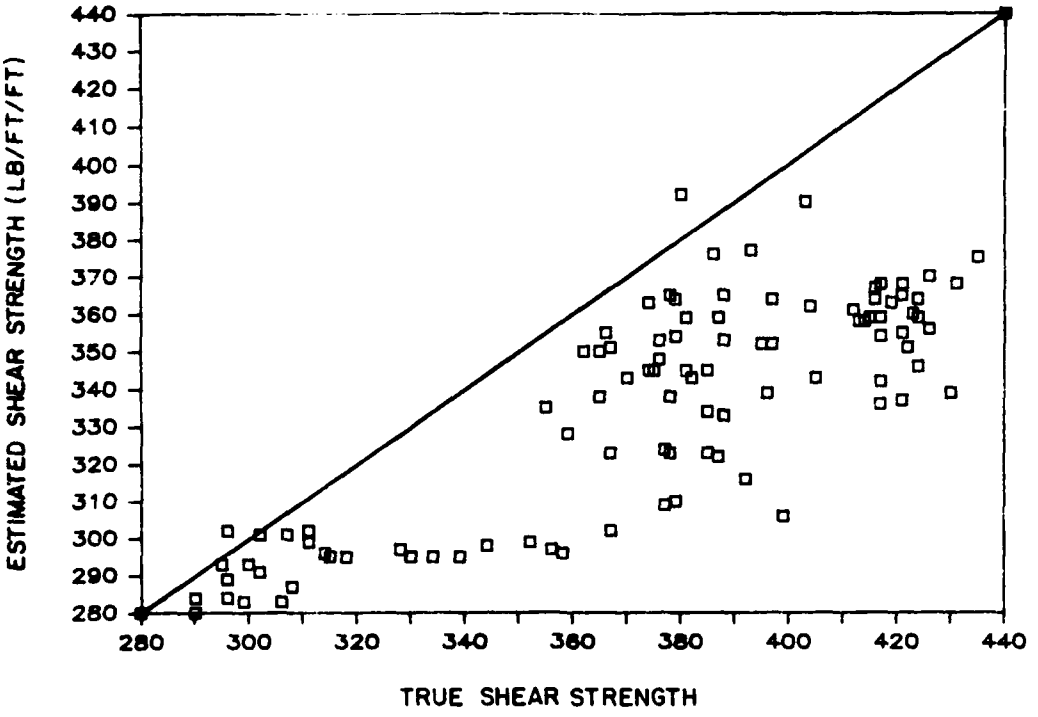

Figure 27. Estimated vs. true shear strength for case 2b.

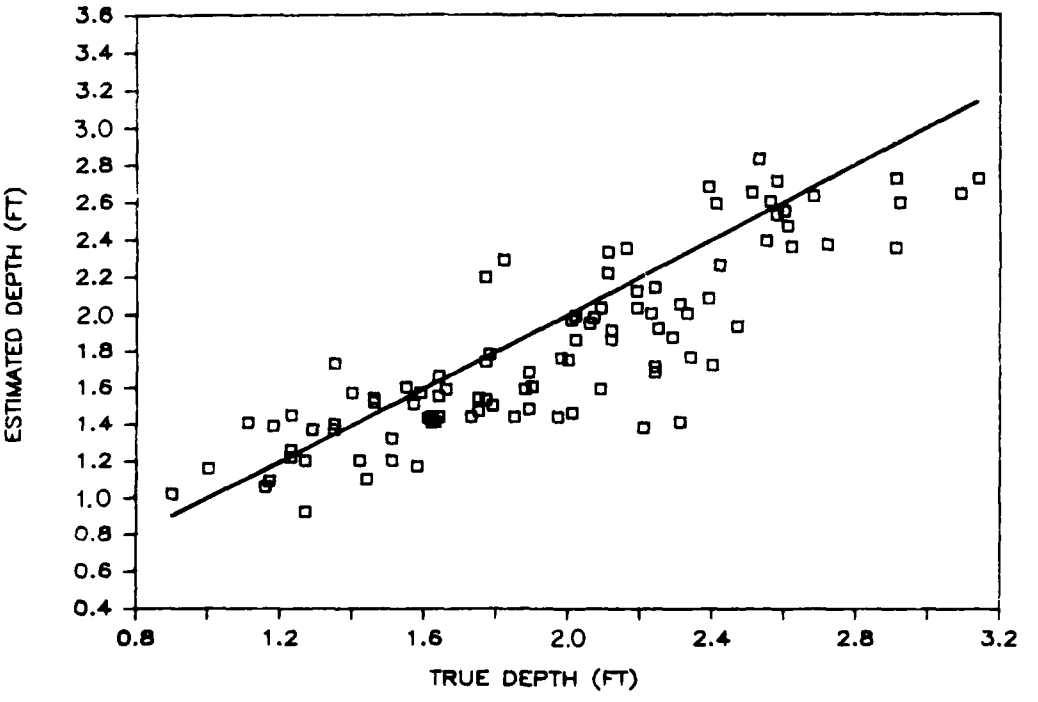

Figure 28. Estimated vs. true depth for case 2b.

Table 3

Effect of Redundant Observation on Estimation Accuracy

v	$(\sqrt{P_\infty})^-$	$(\sqrt{P_\infty})^+_t$	$(\sqrt{P_\infty})^+_e$	% Error
0.071	0.243	0.066	0.068	2.25
0.010	0.243	0.089	0.092	3.70
0.243	0.243	0.162	0.172	6.17
0.316	0.243	0.182	0.192	5.50
0.447	0.243	0.205	0.213	3.90
0.707	0.243	0.224	0.229	2.23

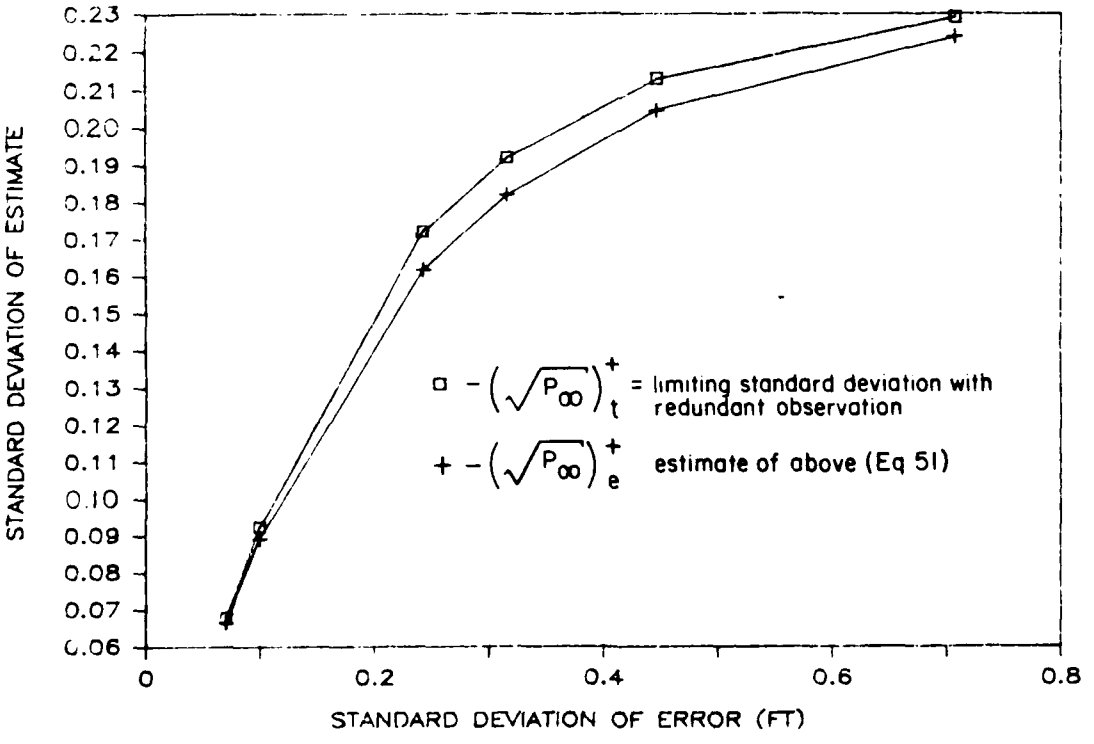

Figure 29. The effect of redundant observation on the accuracy of depth estimation.

APPENDIX:

LIST OF VARIABLES

τ_f	shear stress on the failure surface
c	cohesion intercept; equal to undrained shear strength under assumptions of this report
σ_f	normal stress on the failure surface
ϕ	soil friction angle
F	force on the blade
γ	unit weight of soil
d	depth of cut
q	surcharge on the soil
N_ϕ, N_c, N_q	constants depending on the soil properties, blade roughness, and geometry
B(r)	covariance function at separation distance
σ^2	variance of the fluctuations around the mean
r	distance between any two points
r_o	scale parameter called the covariance distance
E	expectation operator
$B_{cc}(r)$	covariance function of undrained shear strength of soil at separation distance r
ϵ	Gaussian white noise
σ_c^2	variance of undrained soil strength
v(t)	independent Gaussian sequence
$\underline{v}(t)$	vector of independent identically distributed (iid) measurement errors
Ψ	e^{-1/r_o} ; Eq. 12
	n*n one-step transition matrix; Eq 15
$\underline{x}(t)$	n-dimensional state vector
$\underline{u}(t)$	m-dimensional control vector

$\underline{w}(t)$	n-dimensional vector of random perturbation independent Gaussian white noise sequence
Γ	n*m one-step transfer matrix
A,B	arbitrary positive definite matrices
J	performance criterion
L	feedback matrix, depending on A, B, Ψ, and Γ
I	identity matrix
T	matrix transpose
Q	covariance matrix of the depth-of-cut perturbations $\underline{w}(t)$
P_o	initial covariance matrix of the state vector $\underline{x}(o)$
H	deterministic matrix
$\underline{y}(t)$	vector of observations of the states $\underline{x}(t)$
$\underline{g}(.)$	deterministic function
R	covariance matrix of the measurement errors $\underline{v}(t)$
$\hat{\underline{x}}(t)$	mean estimate of $\underline{x}(t)$ conditioned on the measurements $\underline{y}(0), \underline{y}(1),\ldots,\underline{y}(t)$
P_∞	asymptotic variance of the estimated state vector for long lengths of plowing
$\sqrt{P_\infty}$	asymptotic standard error of the estimated state vector for long lengths of plowing

USA-CERL DISTRIBUTION

Chief of Engineers
ATTN: Tech Monitor (10)
ATTN: CEIM-SL (2)
ATTN: CECC-P
ATTN: CECW
ATTN: CECW-O
ATTN: CECW-P
ATTN: CEEC
ATTN: CEEC-C
ATTN: CEEC-E
ATTN: CERD
ATTN: CERD-C
ATTN: CERD-M
ATTN: CERM
ATTN: DAEN-ZCE
ATTN: DAEN-ZCF
ATTN: DAEN-ZCI
ATTN: DAEN-ZCM
ATTN: DAEN-ZCZ

EHSC, ATTN: Library 22060
ATTN: DET III 79906

US Military Academy 10966
ATTN: Facilities Engineer
ATTN: Dept of Geography & Computer Science

AMC - Dir., Inst., & Servc
ATTN: DEH (23)

FORSCOM
FORSCOM Engr, ATTN: Spt. Det.
ATTN: DEH (28)

TRADOC
HQ, TRADOC, ATTN: ATEN-DEH
ATTN: DEH (19)

SHAPE 09055
ATTN: Surv. Section, CCB-OPS
Infrastructure Branch, LANDA

FORT BELVOIR, VA 22060 (11)
ATTN: Canadian Liaison Officer
ATTN: British Liaison Officer
ATTN: Australian Liaison Officer
ATTN: French Liaison Officer
ATTN: German Liaison Officer
ATTN: Water Resources Support Ctr
ATTN: Engr Studies Center
ATTN: Engr Topographic Lab.
ATTN: ATZA-TE-SU
ATTN: ATZA-TE-EM
ATTN: STRBE-BLURE

CRREL, ATTN: Library 03755

WES, ATTN: Library 39180

AFESC, Tyndall AFB, FL 32403

NAVFAC
ATTN: Engineering Command (9)
ATTN: Division Offices (11)
ATTN: Naval Public Works Center (9)
ATTN: Naval Civil Engr Lab. (2)
ATTN: Naval Constr Battalion Ctr

NCEL
ATTN: Library, Code L08A 93043

Defense Technical Info. Center 22314
ATTN: DDA (2)

SETAF Engineer Design Office 09019

Engr Societies Library, NY 10017

Natl Guard Bureau Instl. Div 20310

US Govt Print Office 22304
Receiving Sect/Depository Copies (2)

US Army Env. Hygiene Agency
ATTN: HSHB-E 21010

National Bureau of Standards 20899

158
+2
04/88

END

DATE

FILMED

8-88

DTIC